Analysis of SYGMA Network Inc. Data

by

Lehigh University,
Industrial & Systems Engineering Department,
Enterprise Systems Center (ESC)
Bethlehem, Pennsylvania

On behalf of

WorldKlass Technologies

July 27, 2018

ANALYSIS OF SYGMA NETWORK INC. REFRIGERATED TRAILERS DATA
FOR CAMERON DYNAMICS, LLC dba WORLDKLASS TECHNOLOGIES
BY LEHIGH UNIVERSITY ENTERPRISE SYSTEMS CENTER

INTRODUCTION AND EXECUTIVE SUMMARY

Cameron Dynamics, LLC (dba WorldKlass Technologies) has developed a technology over the past eleven years that has been successfully applied to a wide range of internal combustion engine platforms for the primary purpose of improving fuel economy. This technology is based upon the production of far infrared radiation (photons) in the wavelength range of 3 – 16 microns and bombarding the hydrocarbon fuel with this radiation. The far IR radiation is generated by patented ceramic elements that perpetually, and passively, convert ambient heat energy to light energy (photons).

Fuel economy improvements vary depending on the engine platform and duty cycle, but in general a range of improvement between 4% and 15% has been observed. In addition to early laboratory tests that were performed to validate the physical concept, extensive field testing has been conducted on engine platforms ranging from 60-HP to 6,000-HP and utilizing both diesel fuel and gasoline.

One of these trials conducted by WorldKlass was on a fleet of Sygma Network Inc.'s refrigerated tractor trailers, in particular on the 60-HP diesel engine that is the prime energy source for the refrigeration compressor. This trial extended over a two-year period and included a total of 50 trailers in the test fleet. Initial analysis of the data at the conclusion of the trial indicated a significant reduction in fuel consumption (in excess of 7%) with the portion of the fleet that was equipped with the technology.

Based on these very encouraging initial results, WorldKlass made a decision to engage an objective third-party to perform a detailed statistical analysis of the data to confirm with the highest degree of certainty what results were truly obtained. After some consultation on the matter, the Lehigh University Enterprise Systems Center was retained to perform this statistical study. This report is the end product of this study.

Part 1 of the report reiterates the purpose of the study, and Part 2 provides background information on the parties involved in the initial trial and subsequent analysis. Part 3 of the reports describes the field trial at Sygma Network in greater detail and Part 4 describes the data gathering methodology.

Part 5 of the report outlines the data analysis methodology followed by Part 6, which discusses the results of the data analysis and presents the supporting charts and graphs with associated explanations of their relevance. The conclusions presented in Part 7 summarize the overall fuel efficiency improvement that was observed during the test, and proven to be valid at the highest level of confidence based on the statistical tests applied. Finally, six attachments accompany the report and represent information from which the data gathering and analysis was compiled.

1.0 PURPOSE

This report documents the examination and analysis by the Enterprise Systems Center (ESC) at Lehigh University, as an objective third-party, of data provided by WorldKlass Technologies. The data was captured by Sygma Network, Inc. (Sygma) for refrigerated trailers based at their terminal in Pryor, Oklahoma, during a two-year field trial of the WorldKlass Infrared Fuel Excitation System (the Technology).

2.0 BACKGROUND OF THE PARTICIPANTS

2.1 Cameron Dynamics, LLC dba WorldKlass Technologies

WorldKlass Technologies is a closely held business, headquartered in Allentown, Pennsylvania. WorldKlass holds, through its founders, principals and technology partners, 13 U.S. patents (with one pending) and 12 foreigh patents, regarding beneficial uses of FAR infrared radiation, defined to be infrared light in the wavelength range of 3-20 microns. Laboratory tests at Purdue University in October 2007 demonstrated the validity of the science, and numerous laboratory and field tests starting in 2007 have shown significant improvements in fuel efficiency and reductions in exhaust emissions. (*Infrared Excitation for Hydrocarbon Fuel's Combustion Efficiency*, Purdue University, is provided as Attachment A.) Laboratory and field tests to-date have spanned a variety of diesel engine platforms, and through multiple field tests that have now exceeded eight years in duration the Technology has accumulated over 10 million engine hours of operation without a single adverse incident.

2.2 Lehigh University Enterprise Systems Center

The Enterprise Systems Center (ESC) is a non-profit research center, housed within the Industrial and Systems Engineering (ISE) Department, in the P.C. Rossin College of Engineering and Applied Science of Lehigh University, located in Bethlehem, Pennsylvania. For several decades, the ESC has been a national center of excellence in systems engineering and leadership development through experiential learning.

Since its inception, more than 1,125 research and development projects with over 450 industry partners have been completed by the ESC. More than 4,125 undergraduate and graduate students from the engineering, business and arts/science colleges collaborated to help achieve a high rate of return on investment deliverables. Research efforts are driven by industry needs and historically have been focused in the areas of operations research, analytics, supply chain and logistics, management science, product innovation, sustainability, and agile manufacturing.

The ESC engages students along with professors, senior fellows, subject matter experts, and industry partners, who utilize a layered-mentoring approach. This helps companies use existing or develop new technology tools to grow and compete in a global marketplace. Commonly, research teams are interdisciplinary and engage both undergraduate and graduate students.

2.3 Analytics Team

The analysis effort was led by William Henry (Bill), Senior Fellow. Preliminary work was performed by Lehigh University students, and supervised by Mr. Henry. Bill has over 25 years in statistical modeling and analytic applications with 7 plus years performing Ph.D. level analysis. He is an expert in the development and interpretation of validated standardized instruments for both clinical and business systems using experimental methodology. Bill has SAS proficiency, an R programming certificate, and has worked in SPSS statistics and programing for over 20 years. He has FBI voluntary documentation clearances.

3.0 HISTORY OF THE SYGMA FIELD TRIAL

Field tests at Sygma Network, Inc. of the Technology began during the summer of 2012 at their terminal in Harrisburg, Pennsylvania. In addition to capturing and analyzing data from a test fleet of 83 trailers, Sygma performed tests of their own design, including side-by-side stationary testing over a one-week period.

Based on the favorable results obtained from the Harrisburg tests, a new test was initiated on June 29, 2014 at Sygma's terminal in Pryor, Oklahoma, since it was recognized by Sygma as having a history of reliable data capture. The Oklahoma field trial was designed around a test fleet of 50 trailers, 20 of which would be equipped with the WorldKlass Technology as the Test Group, and 30 of which would remain unequipped as the Control Group. (Representative installation of the Technology on a Thermo King Precedent refrigeration engine is shown in Figure 1.)

Historical data spanning approximately one year was examined to verify that there was adequate consistency in performance among the test fleet trailers and to account for the effects of seasonality. The Technology was installed on the trailers originally identified to be so equipped, 10 being installed on July 25, 2015 and 10 more on August 21, 2015. The test fleet has been monitored since then to identify the difference in performance of the Test and Control Groups.

FIGURE 1 – INSTALLATION OF THE TECHNOLOGY ON THERMO KING MODEL SB

A list of the individual trailers in the equipped Test Group and the unequipped Control Group within the test fleet, is provided in Attachment B.

4.0 DATA COLLECTION METHODOLOGY

4.1 Fuel Dispensed

Gallons of fuel dispensed are tracked at the level of individual fueling transactions for each trailer. Individual transactions include identification of the trailer being fueled, date and time of the transaction, employee dispensing the fuel, and gallons dispensed.

4.2 Engine Hours

Engine hours of operation are tracked for each trailer using meters, which are read when fuel is dispensed. Unlike gallons of fuel dispensed, which are recorded electronically by the fueling system, engine hours are recorded manually, by hand writing the meter reading values on a paper card. These manual entries are color coded with highlighters to identify the week in which the values were read and recorded. (A sample data capture card used to record engine hours is provided in Attachment C.) A single card is used to record data for multiple trailers, and cards are limited to a single reporting "Period" within each fiscal year. (Reporting Periods may be 4, 5 or 6 weeks in duration; reporting Periods are identified in Sygma fiscal year calendars, relevant copies of which are provided in Attachment D.)

4.3 Gallons Per Hour (GPH)

Gallons and hours are each aggregated for each individual trailer for each reporting Period. Data points are established at the Period level, because of challenges in reliably establishing correspondence between gallons and hours at the level of individual fueling transactions and engine hour meter readings, or even at the weekly level. Period level fuel and hours data are combined to calculate gallons per hour (GPH) for each individual trailer for each period. The resultant data set includes these GPH values – some 20 values for Test Group trailers and some 30 values for Control Group trailers – for each Period during the trial. A copy of the data set used in the analysis that is the subject of this report, is provided in Attachment E.

5.0 DATA ANALYSIS METHODOLOGY

Preliminary work was performed by Lehigh University students, and supervised by Bill Henry, during the Fall 2017 semester and again during the Spring 2018 semester, to aggregate, validate and test multiple data sets provided by WorldKlass in their raw form, as originally generated by Sygma.

5.1 Data Aggregation

Data aggregation consisted of compiling Excel spreadsheet files from multiple data sources provided by Sygma, including spreadsheet files of gallons of fuel dispensed and hand-written records of engine hours operated, as described in Section 4.0.

5.2 Data Validation

After receipt and aggregation of the Sygma data, it was validated by identifying anomalous data points, defined as those associated with infeasible values for gallons dispensed and hours accumulated. These anomalous data points are typically the result of a limited number of known causes.

In the case of fuel data, occasionally a fuel pump may shut off automatically during the fueling process, requiring the pump to be reset to complete the fueling process, which causes the fueling system to initiate a second fueling transaction. This results with two transaction records, i.e., two rows of data, with the same trailer number and date, which actually reflect a single fueling transaction. This is illustrated in Figure 2, by the rows highlighted in blue.

Figure 2 – Representative Data Anomalies in Excerpted Portion of Fuel Data File

Trailer Number	TransDate	Quantity	Cumulative Hours	IR	Fuel	Incremental Hours	GPH
6661	4/23/16	10.78	30,440	Yes			
6661	4/25/2016	1.67	30,458	Yes	1.7	18	0.09
6661	4/25/2016	10.36	30,458	Yes	10.4	-	#DIV/0!
6661	4/26/2016	0.47	30,476	Yes	0.5	18	0.03
6661	4/26/2016	13.02	30,476	Yes	13.0	-	#DIV/0!
6661	4/27/2016	11.36	30,493	Yes	11.4	17	0.67
6661	4/29/2016	12.00	30,501	Yes	12.0	8	1.50
6661	5/1/2016	20.10	1,234	Yes	20.1	(29,267)	(0.00)
6661	5/6/2016	17.69	30,566	Yes	17.7	29,332	0.00
6661	5/7/2016	15.96	30,591	Yes	16.0	25	0.64
6661	5/8/2016	21.00	30,610	Yes	21.0	19	1.11
6661	5/9/2016	0.58	30,624	Yes	0.6	14	0.04
6661	5/9/2016	9.70	30,624	Yes	9.7	-	#DIV/0!
6661	5/11/2016	12.08	30,638	Yes	12.1	14	0.86
6661	5/11/2016	7.52	30,650	Yes	7.5	12	0.63
6661	5/13/2016	24.04	30,669	Yes	24.0	19	1.27
6661	5/16/2016	25.14	30,705	Yes	25.1	36	0.70
6661	5/19/2016	23.18	30,731	Yes	23.2	26	0.89
6661	5/21/2016	13.46	31,852	Yes	13.5	1,121	0.01
					225.9	291.0	0.78

The second example involves erroneous hours readings. This may occur unintentionally, such as when a value is an order of magnitude smaller than the values recorded before and after but has similar digits. It may also be the result of an apparently intentional "shortcut", when someone records simplified values such as "9999" or "1234", as illustrated in Figure 2 and highlighted in yellow. In both of these highlighted examples, the remedy is to combine the erroneous data row with an adjacent valid row, to create a new single data point. Additionally, a more advanced statistical process can be used by engaging the statistical program's algorithm designed for missing data replacement, however this was not deemed necessary for the present analysis.

Another source of anomalous data is fueling transactions in which two different trailer numbers are included in a single fueling transaction. This is understood to result from the employee dispensing the fuel not resetting the fuel pump after filling a trailer, and then proceeding to fill the next adjacent trailer. In these circumstances, the fuel dispensed is assumed to have been divided equally between the two identified trailers, unless the total amount of fuel listed as being dispensed to the two trailers is de minimis, in which case the identified amount of fuel is ignored.

5.3 Data Testing

The data testing effort consisted of three general elements: data reliability and normality; spreadsheet analyses; and, complex modeling.

Data Reliability and Normality – Before the data could be analyzed, it was necessary to determine whether the data can be relied upon reasonably. This was accomplished by evaluating the normality of the data. For the Sygma data, the normality of the values for gallons of fuel dispensed and engine hours operated were tested, as were the calculated gallons per hour (GPH) values - for the Control Group and the Test Group, separately for the periods prior to and after the installation of the Technology on the trailers in the Test Group. Results of tests of the normality of the GPH values are provided in Attachment E. In order to calculate correlations, regression analysis and parametric or non-parametric analysis, the assumptions of normality must be met. The Levene statistical test for normality on each of the individual periods in the years 2015-2016-2017 proved to be significant. With the assumptions of normality met, meaning that each data set falls into acceptable parameters of the central limit theorem, further statistical analysis can be relied upon.

Modeling Using SAS, SPSS and R – A series of analyses were performed using SAS and SPSS. Collaboration with statistician colleagues outside ESC resulted in additional analyses being performed by programming in R. Both ESC and the outside colleagues found similar statistical trends and results, as described in Section 6.2.

ESC always employs the latest versions of SAS, SPSS and R in its analyses. These data mining and statistical programs use advanced algorithms for statistical modeling. These programs are recognized as a best practice methodology in research relating to clinical and pharmacology, genetics, engineering and data sciences.

6.0 DATA ANALYSIS AND RESULTS OBTAINED

The analysis consisted of two broad steps: testing to evaluate normality of the data; and, evaluating differences between the fuel efficiency of the Test Group and Control Group, prior to and after installation of the WorldKlass Technology.

- The normality of the data was evaluated using T-Tests[1], examination of standard deviations using the Pooled Standard Error (PSE)[2] and Satterthwaite Approximation[3], Levene's Tests[4], and Shapiro-Wilks Tests[5].
- The data were evaluated using SAS, SPSS and R to generate a broad array of statistical metrics, based upon which comparisons could be made between the Test Group and the Control Group.

6.1 Data Reliability and Normality

The data was examined using SAS for the Control Group and for the Test Group during the Periods prior to the installation of the Technology and after the installation. The frequency plots in Figure 3 include the Test Group (Equipped) and the Control Group (Unequipped) and the frequencies of values in defined GPH ranges, during the post-installation portion of the trial. The Gaussian kernel curve[6] is a method of smoothing the data and is often used to observe normality issues visually. Both the normal and the Gaussian kernel curves are fitted to the actual data, and are overlaid for comparison.

FIGURE 3 – CONTROL AND TEST GROUPS GPH VALUE FREQUENCY PLOTS

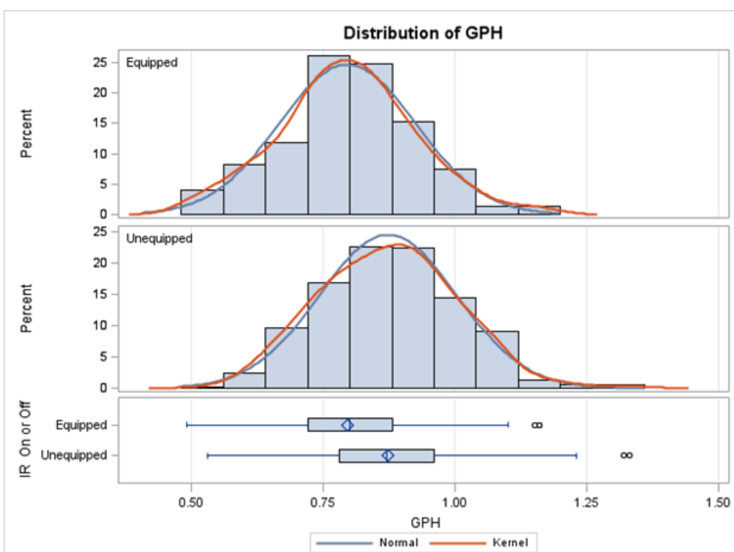

In Figure 4, SAS statistical outputs are provided, that include pooled and Satterthwaite T-Tests, for which the P values[7] are less than 0.0001, which is indicative of a very high degree of correlation.

FIGURE 4 – SAS STATISTICAL OUTPUTS

IR On or Off	N	Mean	Std Dev	Std Err	Minimum	Maximum
Equipped	230	0.7950	0.1295	0.00854	0.4900	1.1600
Unequipped	375	0.8724	0.1303	0.00673	0.5300	1.3300
Diff (1-2)		-0.0773	0.1300	0.0109		

IR On or Off	Method	Mean	95% CL Mean		Std Dev	95% CL Std Dev	
Equipped		0.7950	0.7782	0.8119	0.1295	0.1186	0.1425
Unequipped		0.8724	0.8591	0.8856	0.1303	0.1216	0.1403
Diff (1-2)	Pooled	-0.0773	-0.0987	-0.0559	0.1300	0.1230	0.1377
Diff (1-2)	Satterthwaite	-0.0773	-0.0987	-0.0560			

Method	Variances	DF	t Value	Pr > |t|
Pooled	Equal	603	-7.10	<.0001
Satterthwaite	Unequal	486.67	-7.11	<.0001

Equality of Variances

Method	Num DF	Den DF	F Value	Pr > F
Folded F	374	229	1.01	0.9283

The standard deviations were examined using the Pooled Standard Error (PSE) and Satterthwaite Approximation, yielding similar results. The arithemetic average (PSE) and weighted average (Satterthwaite) yielded the same value of 0.0773 for the difference between the equipped and unequipped means. Both the pooled variance metric and the Satterthwaite (S-W) metric are methods for statically organizing variables of different sizes. The probability output should be statically significant in order to consider the overall statistical integrity of the observations.

Levene's Test was also applied to calculated GPH values determine whether variances are equal across Periods, separately for the Control Group and the Test Group, for each of the 25 Periods included in the trial. The Levene's Test indicates that the data is sufficiently normal to be relied upon. These values are presented in Attachment F.

Students during Spring 2018 Semester looked at Shapiro-Wilks testing regarding normality; results of the Shapiro-Wilks tests are presented in Section 6.2.

Based on these results, the Sygma data may be relied upon with high confidence.

6.2 Modeling Using SAS, SPSS and R

Using SPSS Modeler/Statistics, the calculated GPH values were examined for both the Control Group and the Test Group, both for the eleven Periods prior to installation of the Technology, and the fourteen Periods after installation. In the following tables and graphs the outputs observations on the particular year's statistical metrics are provided. These show the t scores with related metrics, the normality of the data, the and the nature of the data's shape in descriptive observations. The results are shown in Figures 5 through 8.

FIGURE 5 – TEST GROUP PRIOR TO TECHNOLOGY INSTALLATION

One-Sample Test

	Test Value = 0					
					Interval of the	
	t	df	Sig. (2-tailed)	Mean Difference	Lower	Upper
No_IR_2015_Test Group	64.523	230	.000	.89758	.8702	.9250

Tests of Normality

	Shapiro-Wilk		
	Statistic	df	Sig.
No_IR_2015_Test Group	.767	231	.000

Descriptive Statistics

	N	Mean	Variance	Skewness	Kurtosis
	Statistic	Statistic	Statistic	Statistic	Statistic
No_IR_2015_Test Group	231	.8976	.045	3.957	35.757

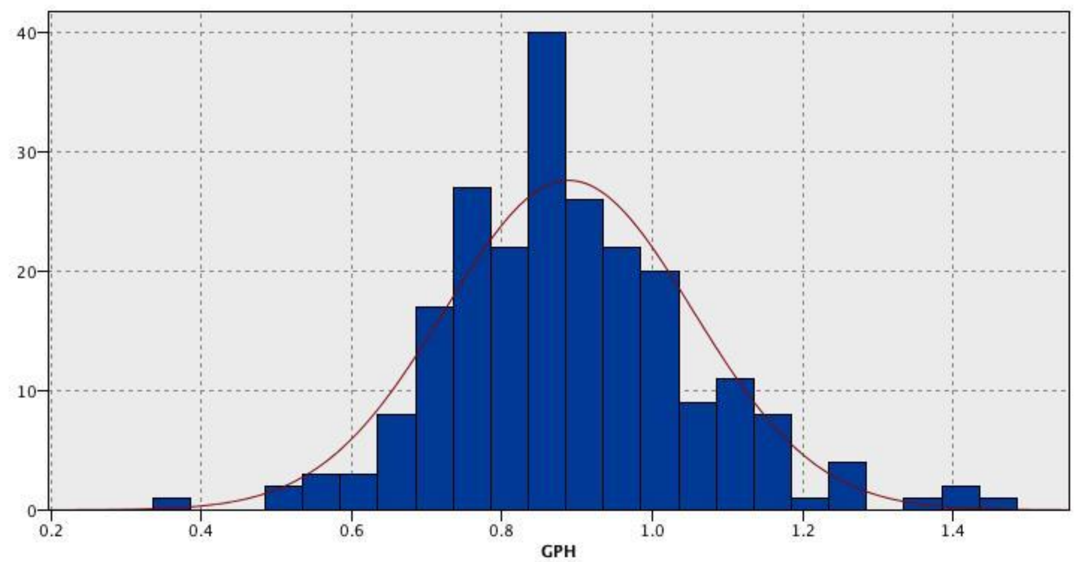

The t score for the 2015 test group having no IR is positive, t=64.5, with a strong significance probability value of .001. The overall mean differences in this set of data are about 0.9 with the lower and upper values being 0.87 and 0.93 respectively. The degrees of freedom, df, is calculated to be 230. The normality of this data set is significant with a probability value of less than .001. This indicates that the data is not normal, although the shape of the histogram graph clearly shows that the data is heading in that direction. This data is positively skewed with a large kurtosis of 35.8 indicating a significant number of the data is represented in the distribution tails.

FIGURE 6 – CONTROL GROUP PRIOR TO TECHNOLOGY INSTALLATION

One-Sample Test

	Test Value = 0					
					Interval of the	
	t	df	Sig. (2-tailed)	Mean Difference	Lower	Upper
No_IR_2015_Control Group	61.393	329	.000	.89591	.8672	.9246

Tests of Normality

	Shapiro-Wilk		
	Statistic	df	Sig.
No_IR_2015_Control Group	.625	231	.000

Descriptive Statistics

	N	Mean	Variance	Skewness	Kurtosis
	Statistic	Statistic	Statistic	Statistic	Statistic
No_IR_2015_Control Group	330	.8959	.070	5.939	67.054

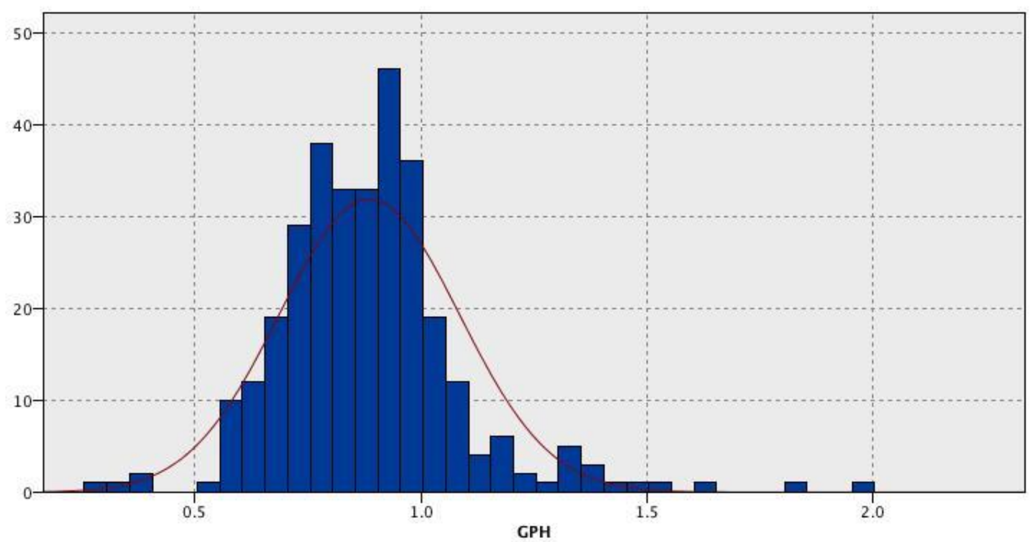

Regarding Figure 6, the t score for the 2015 control group having no IR is positive, t=61.4, with a strong significance probability value of .001. The overall mean differences in this set of data are about 0.9 with lower and upper values being 0.87 and 0.94 respectively. The degrees of freedom, df, is calculated to be 329. The normality of this data set is significant with a probability value of less than .001. This indicates that that the data is not normal, although the shape of the histogram graph clearly shows that the data is heading in that direction. This data is positively skewed with a large kurtosis of 67.1 indicating a significant number of the data is represented in the distribution tails.

FIGURE 7 – TEST GROUP AFTER TECHNOLOGY INSTALLATION

One-Sample Test

	Test Value = 0					
					Interval of the	
	t	df	Sig. (2-tailed)	Mean Difference	Lower	Upper
IR_2016_Test Group	97.009	230	.000	.80078	.7845	.8170

Tests of Normality

	Shapiro-Wilk		
	Statistic	df	Sig.
IR_2016_Test Group	.993	231	.317

Descriptive Statistics

	N	Mean	Variance	Skewness	Kurtosis
	Statistic	Statistic	Statistic	Statistic	Statistic
IR_2016_Test Group	231	.8008	.016	-.139	-.202

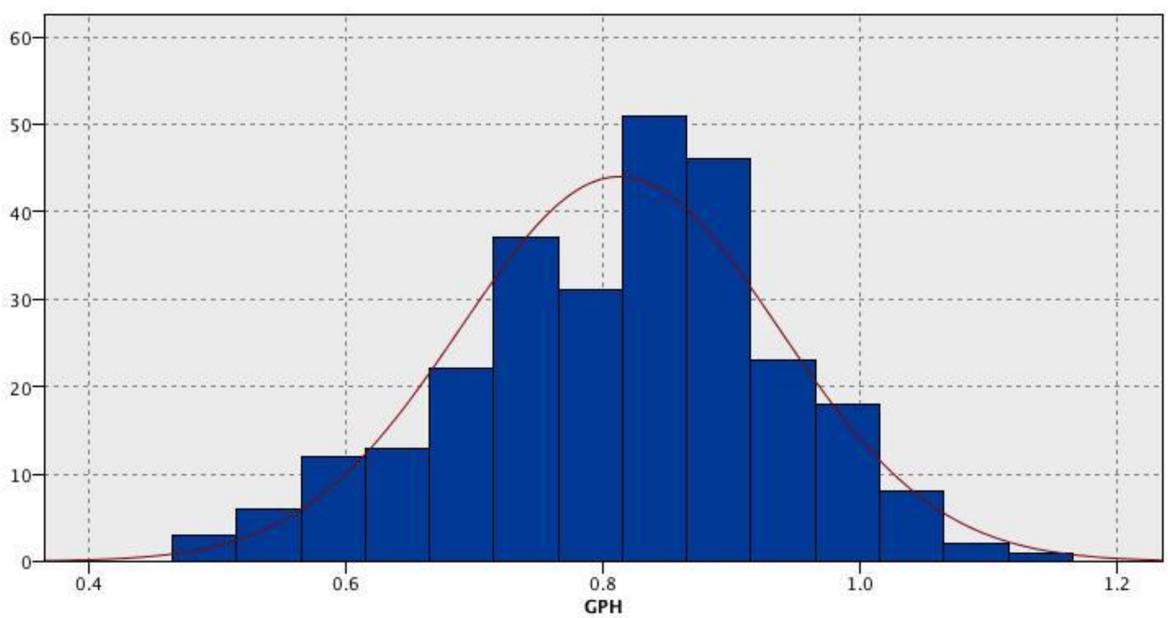

Regarding Figure 7, the t score for the 2016 test group having IR is positive, t=97 with a strong significance probability value of .001. The overall mean differences in this set of data are about 0.8 with the lower and upper values being 0.78 and 0.82 respectively. The degrees of freedom, df, is calculated to be 230. The normality of this data set is not statistically significant with a probability value of 0.317. This indicates that that the data is normal, the shape of the histogram graph shows that the data is fitting close within the Gaussian bell curve. This data is negatively skewed with a small negative kurtosis of 0.2 indicating that most of the data are represented between the extremes of the distribution tails .

FIGURE 8 – CONTROL GROUP AFTER TECHNOLOGY INSTALLATION

One Sample Test

	Test Value = 0					
					Interval of the	
	t	df	Sig. (2-tailed)	Mean Difference	Lower	Upper
No_IR_2016_Control Group	123.350	329	.000	.86521	.8514	.8790

Tests of Normality

	Shapiro-Wilk		
	Statistic	df	Sig.
No_IR_2016_Control Group	.990	231	.108

Descriptive Statistics

	N	Mean	Variance	Skewness	Kurtosis
	Statistic	Statistic	Statistic	Statistic	Statistic
No_IR_2016_Control Group	330	.8652	.016	.299	.413

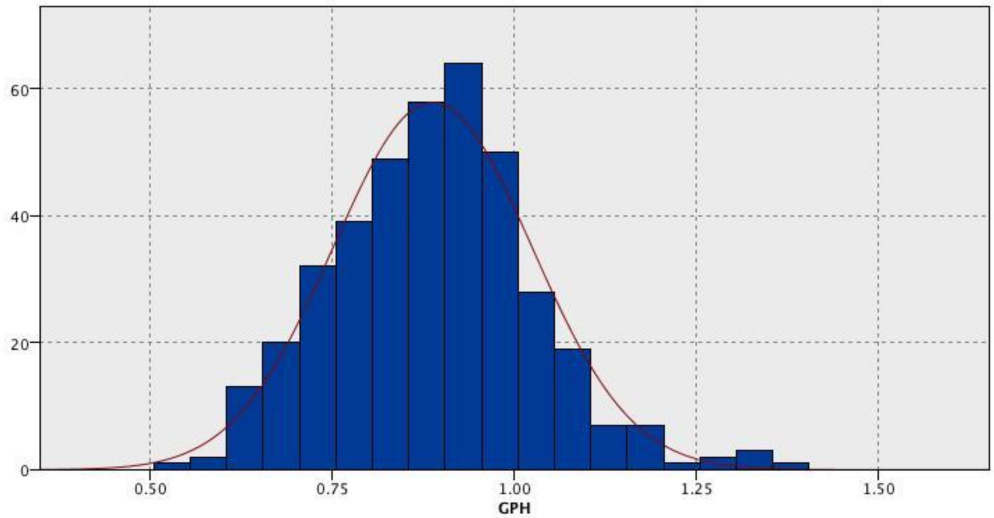

Regarding Figure 8, the t score for the 2016 control group having no IR is positive, t=123.4 with a strong significance probability value of .001. The overall mean differences in this set of data are about 0.9 with the lower and upper values being 0.85 and 0.88 respectively. The degrees of freedom, df, is calculated to be 329. The normality of this data set is statistically significant with a probability value of .108. This indicates that the data is normal, the shape of the histogram graph shows that the data is fitting close within the Gaussian bell curve. This data is positively skewed with a small negative kurtosis of 0.4 indicating that most of the data are represented between the extremes of the distribution tails.

Logarithmic regression modeling is often used in industrial engineering and biological sciences and other fields. This analytical method creates both a statistical metric and a graphical visual. The solid line that is generated is the trend line of the data flow for a given set of variables. The points in the plot provided in Figure 9 are the actual data for the variables. The regression of the data to the mean, also known as least squares, shows how the data is structured and how far a given point strays from the regression line. The graphical output is often an excellent way to detect anomalies in the data set. It is also a visual way to observe the differences between sets of data.

Observing the regression lines generated by SAS using the logs of the Sygma data for the Control Group with no IR (blue) and the Test Group (red), it is clear to see that there are significant differences. Both the X and Y axes are reconfigured with increments reflecting the frequency and a simplified magnitude. The X axis represents the frequency of ranges of logarithms of GPH values for both sets of data while the Y axis is a logs of GPH magnitude scale. The convergence of the two lines is where both the Control Group and the Test Group, historically, had no IR technology. The two regression lines begin to separate after the IR technology was installed. As the lines progress the separation in fuel consumption, expressed in GPH values, becomes even more pronounced.

FIGURE 9 – LOGARITHMIC REGRESSION ANALYSIS USING SAS – TREND LINE

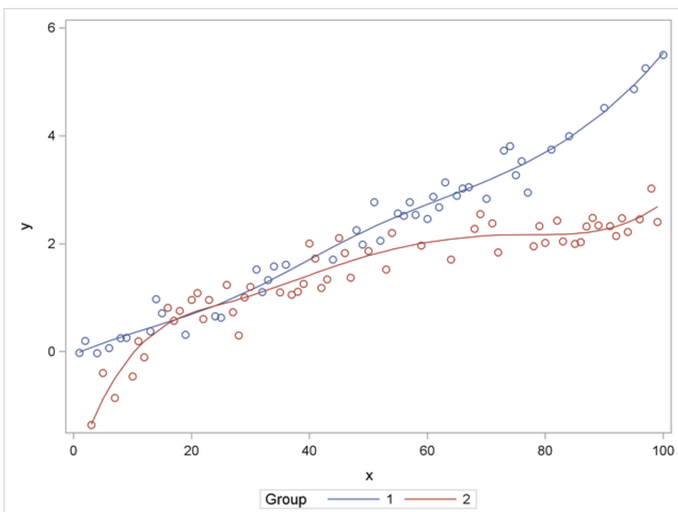

In the regression analysis table provided in Figure 10, it is important to note the standard error, or variance, in the data is less in the Test Group. This would indicate the variability in the GPH consumption decreases with the use of the IR Technology. The decrease in variability suggests that the engines that are exposed to the Technology are running more consistently and predictably.

FIGURE 10 – LOGARITHMIC REGRESSION ANALYSIS USING SAS – METRICS

Estimates					
Label	Estimate	Standard Error	DF	t Value	Pr > |t|
Group 1, x=20	0.6915	0.09546	86	7.24	<.0001
Group 2, x=20	0.7175	0.07953	86	9.02	<.0001
Diff at x=20	-0.02602	0.1243	86	-0.21	0.8346

Logarithmic regression modeling is often used in industrial engineering and biological sciences and other fields. This analytical method creates both a statistical metric and a graphical visual. The solid line that is generated is the trend line of the data flow for a given set of variables. The points in the plot provided in Figure 9 are the logs of the actual data for the variables. The statistical method of logarithmic regression analysis statistically refines the data, "smoothing" the visual observations. The regression of the data to the mean, also known as least squares, shows how the data is structured and how far a given point strays from the regression line. The graphical output is often an excellent way to detect anomalies in the data set. It is also a visual way to observe the differences between sets of data.

Observing the regression lines generated by SAS using the logs of the Sygma data for the Control Group with no IR (blue) and the Test Group (red), it is clear to see that there are significant differences. Both the X and Y axes are reconfigured with increments reflecting the frequency and a simplified magnitude. The X axis represents the frequency of ranges of logarithms of GPH values for both sets of data while the Y axis is a logs of gph magnitude scale. The convergence of the two lines is where both the Control Group and the Test Group, historically, had no IR Technology. The two regression lines begin to separate after the IR Technology was installed. As the lines progress the separation in fuel consumption, expressed in GPH values, becomes even more pronounced.

7.0 CONCLUSIONS

7.1 Fuel Efficiency Benefit

The data show that prior to the installation of the WorldKlass Infrared Fuel Excitation System, the two groups of trailers – one "to be equipped" and the other to remain unequipped as a control – are statistically similar, averaging 0.89 GPH and 0.81 GPH respectively. After equipping the test group of 20 trailers with the Technology, the performance of the two groups diverged, and remained separated by a difference in average standardized t score of 24.1% over the subsequent year, as shown in Figure 11. In statistics, t-scores standardize comparative groups of values and convert them into a statistical format. The reason for converting comparative groups into standardized scores involves equalizing their variances so that they have an equal statistical metric base. The p-values in the table are less than .000 which is a robust statistical confidence level indicating that this difference between the two groups, the 2016 Control Group and the 2016 Test Group, are not a chance event. Based upon this standardized comparison, it can be stated, with better than 95% confidence, that an improvement in fuel efficiency between 7.9% and 11.2% is real and is the result of application of the WorldKlass Infrared Fuel Excitation System.

FIGURE 11 – ONE-SAMPLE TEST POST INSTALLATION OF WORLDKLASS TECHNOLOGY

One-Sample Test

	Test Value = 0					
					Interval of the	
	t	df	Sig. (2-tailed)	Mean Difference	Lower	Upper
No_IR_2016_Control Group	121.111	318	.000	.86417	.8501	.8782
IR_2016_Test Group	97.009	230	.000	.80078	.7845	.8170

Figure 11, above, provides an observation between the statistically significant t-scores. This standardized score shows a difference of 24.102, demonstrating close to two standard deviations of separation. The p-values in the table are less than .000 which is a robust statistical confidence level indicating that this difference between the two groups, the 2016 Control Group and the 2016 Test Group, are not a chance event.

ENDNOTES

1) T-Tests – A t score is a standardized scoring process which converts a group of scores, or a single score, into a common format by which other standardized scores can be compared. This statistic is based upon the central limit theorem which is a statistical theory that helps define the governing rules of evaluating a given data population. A t score is utilized when the absolute number of a data population is not known. T scores have a mean of 50 and a standard deviation of 10. A t a score of 100 is 5 standard deviations away from the mean. Positive or negative t scores indicate which direction a score is heading and are not necessarily to be interpreted as good or bad. T scores are used extensively in experimental modeling, probability and hypothesis testing.

2) Pooled Standard Error (PSE) – The standard error of a dataset is based upon a data sampling. It is called a sampling because it is not presumed to be an absolute complete compiling of all possible data, historically or in the future. The standard error is similar to the standard deviation of a dataset.

A pooled standard error takes into account two or more sample variables and "pools" the standard errors of those variables together for an adjusted statistical metric.

3) Satterthwaite Approximation – The Satterthwaite approximation, or the Welch–Satterthwaite (W-S) equation, is applied when multiple datasets have differing numeric counts. For example, a dataset of 125,000 can be statistically compared to a dataset of 101,000 with statistical confidence using the W-S, because it assumes the populations being compared are not equal. The differing numeric counts of the multiple data variables are pooled together for the statistical modeling processes.

4) Levene's Tests – Levene's Tests check a group of data variables for variance commonalities. If a number of data variables have the statistically same variances, then restrictions are placed upon statistical modeling. The Levene test is a probability hypothesis that a set of variables are not the same. Probability values are generated and used to determine the likelihood of common variances. The stated null hypothesis of the Levene test is that the test groups are similar. If the probability value indicates that the null hypothesis is not true, then the datasets do not have like variances.

5) Shapiro-Wilks Tests – The Shapiro-Wilks Tests looks for normality in a dataset. Probability values are generated in this test for normality to be determined. Whether the null hypothesis should be rejected or the alternative hypothesis accepted is determined by an acceptable p value. A normal distribution conforms to the central limit theorem. The probability alpha value for the Shapiro-Wilks test, like most probability alpha levels, is $p <= .05$.

6) Normality and Gaussian kernel curve – Normality in a dataset is crucial in that it determines what type of statistical method can be applied and which one(s) will give false significance. The normality of a set of data means that it is conforming to the statistical probability model of the central limit theorem. Most often, if a dataset is meeting the requirements of the central limit theorem the histogram of that data's frequency distribution will have a "bell" shape. The Gaussian kernel is a smoothed bell-shaped line of a dataset. In many statistical programs the exact bell shape will be presented along with the data's kernel density approximation. This kernel approximation line is based upon a nonparametric probability density test of the data and is often more accurate than the basic rendered bell shape.

7) p-values – In probability, hypothesis testing requires a criteria statistic known as an alpha level. A null hypothesis states that there is no difference between dataset "a" and dataset "b" and an alternative hypothesis states that the difference between groups of datasets are statistically different. Testing the difference between groups of datasets requires a statistical metric, the p value. The probability that a desired hypothesis test outcome is not the result of some element of chance or dataset anomaly is what the p value does. After it is determined that a dataset has met the assumptions of the central limit theorem, a p value is used in a statistical modeling process. Most rigorous academic schools agree that a p value of $p<=.05$ should be achieved as an acceptable alpha level. However, very small p values, $p<=.001$ are considered meaningfully better in some testing environments such as pharmaceutical effectiveness. P values in hypothesis testing that are greater than $p<= .05$ are considered evidence that a null hypothesis should be accepted.

LIST OF ATTACHMENTS

A – Infrared Excitation for Hydrocarbon Fuel's Combustion Efficiency, Purdue University

B – Sygma Test Fleet Trailers

C – Sygma Engine Hours Data Capture Card (Representative Sample)

D – Fiscal Calendars (2015, 2016 and 2017)

E – Sygma Oklahoma Test Data (P15-1 Through P17-2)

F – T-Test Results [File= OUTPUT T scores 2015-2016.xlsx]

ATTACHMENT A

Infrared Excitation for Hydrocarbon Fuel's Combustion Efficiency, Purdue University

This paper was presented to the 3rd Emission Solutions in Transportation,
AFS International Conference, Oct. 25 - 27, 2007, Ann Arbor, Michigan, U.S.A.

Infrared-Excitation for Improved Hydrocarbon Fuel's Combustion Efficiency

Albert C. Wey
Aldi Far-Infrared Products, Inc.

Rodney G. Handy
Dept. of Mechanical Engineering Technology
Purdue University

Yuan Zheng and Chul H. Kim
Maurice J. Zucrow Laboratories
Purdue University

ABSTRACT

Photoexciting hydrocarbons with infrared shorter than 20 microns in wavelengths for enhanced fuel conversion efficiency are believed to be scientifically predictable. This paper describes a scientific investigation in the concept using infrared excitation for increased hydrocarbon fuels' combustion efficiency. The IR-effect on flame structure is studied in a widely-used counterflow methane-air diffusion flame experiment. Species concentrations for H_2, O_2, N_2, CH_4, CO, CO_2, C_2H_2, and C_2H_4 across the flame were measured using sampling and gas chromatography while NO (nitric oxide) concentrations were measured using chemiluminescence analysis. The experimental results indicate IR-excitation makes fuel more combustible and burn faster than regular fuel. As a result of faster combustion, the fuel consumption rate and peak CO and NO emissions are reduced. IR-excitation was applied in several engine and vehicle tests to examine its effects on improving engine efficiency. The results suggest IR-excitation can significantly improve engine performance for increased fuel economy and reduced emissions.

INTRODUCTION

Using infrared-excited fuels for improved fuel efficiency of internal combustion engines was first disclosed in 2003 [1]. Hydrocarbons are IR-active and absorb multi-photons in 3 – 14 μm wavelengths, causing molecular vibrations [2]. Photochemistry enhancement of reaction rates by reactant vibrational excitation have been demonstrated in laboratory dynamics studies [3]. These scientific facts suggest that by IR-exciting hydrocarbon fuels combustion efficiencies will be significantly enhanced. Though photoexciting hydrocarbon molecules for enhanced fuel conversion efficiency are believed to be scientifically predictable, a broadband IR-excitation source that could facilitate the proposed applications did not commercially exist. Adopting the IR technology that prevailed in Japan, we engineered an IR-ceramic from selective transition metal oxides that emit 3 - 14 μm wavelength mid-infrared [4]. In engine applications, the IR-emitting ceramic can be clamped to the exterior of a nonmetal supply fuel line, since 3 – 14 μm wavelength photons can penetrate nonmetal materials. Hydrocarbons traversing thorough the fuel line are exposed to infrared radiation and excited before the fuel enters cylinders for combustion. Confirmatory test results demonstrating IR-effect on improving engine performance to significantly improve fuel economy and emissions were reported [5]. In that report, all targeted emissions from engines, including THC, CO, and NOx, were simultaneously reduced. Nevertheless, how IR-excitation participates in the thermochemical process of combustion to improve fuel's conversion efficiency remains unidentified.

The combustion of multi-component commercial fuels (e.g. gasoline, diesels) in an engine involves many complicated processes, such as atomization, evaporation, turbulent mixing, and combustion timing. To eliminate the complexities in a gasoline or diesel engine, laminar non-premixed counterflow methane-air flame experimentation was used at Zucrow Laboratories, Purdue University to investigate the IR-effect on combustion of methane, the simplest form of hydrocarbon fuel, in the present study. Counterflow flames are widely used in evaluation of chemical kinetic rates because they are one-dimensional and have a uniform strain rate [6]. Counterflow flames also allow the use of OPPDIF code developed by Sandia [7,8] to reveal chemical kinetics details with manageable computational times. Besides, the methane mechanism and the thermochemical database given in GRI-Mech 2.11 [9] can be used to predict and compare the measured concentrations of major species in the flame.

The present study has successfully demonstrated the IR-excitation effect on influencing methane flame structure (i.e. distribution of species across the flame) with reduced pollutant (CO, and NO) emissions. Preliminary results are very encouraging, indicating the IR-effect is existent. The IR-effect was verified on a single-cylinder engine to reduce CO and NOx and on a Ford F-350 diesel truck to simultaneously reduce fuel consumption and emissions. In this paper the hypothetical model is described and results are presented.

ABSORPTION OF INFRARED RADIATION

When a photon is absorbed by a molecule, it ceases to exist and its energy is transferred to the molecule. This energy can be transferred to vibrational, rotational, electronic, or translational forms. Excitation of vibrational modes in a molecule requires a photon with wavelength typically shorter than 20 µm. Examination of the geometry of the molecule can tell if a molecule will be infrared-active. Hydrocarbons are IR-active and absorb IR photons to cause molecular vibrations. Some exemplary IR-excited vibrations in hydrocarbons are listed in Table 1.

Table 1. IR absorptions by hydrocarbon molecules.

ω (cm^{-1})	λ (µm)	Bond Structure
1315 – 1475	6.78 – 7.60	C–H (in *alkanes*)
2800 – 3000	3.33 – 3.57	C–H (in *alkanes*)
1450 – 1600	6.25 – 6.90	C=C bond in *aromatic ring*
1650 – 1670	5.99 – 6.06	C=C
2100 – 2260	4.42 – 4.76	C≡C
3000 – 3100	3.23 – 3.33	C–H (part of *aromatic ring*)
3300	3.03	C–H (C is *acetylenic*)
3020 – 3080	3.25 – 3.31	C–H (C is *ethylenic*)
1420–1470	6.80–7.04	Alkanes' $-CH_3$
1375	7.27	Alkanes' $-CH_3$
1430–1470	6.80–6.99	Alkanes' $=CH_2$
1370, 1385	7.30, 7.22	Alkanes' $-CH(CH_3)_2$
1170	8.55	Alkanes' $-CH(CH_3)_2$
1370, 1395	7.30, 7.17	Alkanes' $-C(CH_3)_3$
910–920	10.87–10.99	*Alkenes' $RCH=CH_2$
990–1000	10.00–10.10	*Alkenes' $RCH=CH_2$
880 – 900	11.11–11.36	*Alkenes' $R_2C=CH_2$
675 – 730	13.70–14.81	*Alkenes' RCH=CHR *cis*
965 – 975	10.26–10.36	*Alkenes' RCH=CHR *trans*
730 – 770	12.99–13.70	*Aromatic C–H (1)
735 – 770	12.99–13.61	*Aromatic C–H (2) *ortho*
690 – 710	14.08–14.49	*Aromatic C–H (2) *meta*
750 – 810	12.35–13.33	*Aromatic C–H (2) *meta*
810 – 840	12.35–11.90	*Aromatic C–H (2) *para*

* means "Out-of-Plane"; (1) Mono-substituted; (2) Distributed.

For example, the C≡C bond in hydrocarbon molecule has a higher force constant than C=C bond so that C≡C bond absorbs IR at a higher frequencies (i.e. higher energy) at 2100 – 2260 cm^{-1} (or 4.76 – 4.42 µm wavelengths) than the C=C bond at 1650 – 1670 cm^{-1} (6.06 – 5.99 µm). It takes more energy to make the stronger C≡C bond vibrate than it does to the C=C bond. Organic chemists have been using the IR absorption spectral information (called Infrared Correlation Charts) to identify hydrocarbon specimens for many decades [10].

MOLECULAR VIBRATIONS

Photoselective Chemistry is concerned with the influence of selective optical excitation on the acquisition, storage and disposal of energy and on the reactivity of molecules. Classic work of Evans and Polanyi in the 1930s illustrated the importance of molecular vibrational energy in reaction dynamics [11]. It was recognized early in the study of chemical kinetics that increasing the energy of reactants increased reaction rate, which was usually accomplished by simply raising the reaction temperature. However, Evans and Polanyi presented the argument that the reactant vibrational energy is the most effective at promoting reaction. As experimental techniques were refined, it became possible to demonstrate that increasing vibrational energy is indeed relatively more important than raising temperature in enhancing a molecular reaction. The expectation is that if vibrational excitation is sufficient to raise the system and lower the activation barrier, substantial rate enhancement would be realized.

Tunable lasers provide a very convenient method for obtaining selective vibrational excitation. A number of reactions of IR laser-excited species have been studied. The correlation between ground-state heats of reaction and vibrationally induced reaction rate enhancement is striking for these processes. Vibrational energy in some of these cases was found to enhance the reaction rate by two orders of magnitude [12]. It is concluded that chemical reactions can be drastically enhanced by optical excitation from infrared lasers.

INFRARED MULTIPHOTON ABSORPTION AND EXCITATION

The discovery that polyatomic molecules under collision-free conditions may absorb many infrared quanta from an IR laser had generated interests regarding molecular multiphoton process (MMP). Based on the currently available experimental information and theoretical studies, a qualitative picture can be drawn as in Fig.1 [13]:

The molecular energy levels can be separated into three regions [14]. In the lowest energy range (region I) the density of molecular states is very low and the IR field is interacting with isolated molecular states. In this region, multi-photon resonances are accounted for in terms of the molecular level-scheme of region I.

After the molecule absorbs a few quanta, the density of molecular states becomes very large, and we can no longer describe the time evolution in terms of few isolated molecular states. This region is denoted region II, quasi-continuum, involving intramolecular energy transfer and line broadening (dephasing).

Finally, when the molecule has acquired enough energy for dissociation, it enters the region III, where we have to incorporate the dynamics of unimolecular decomposition.

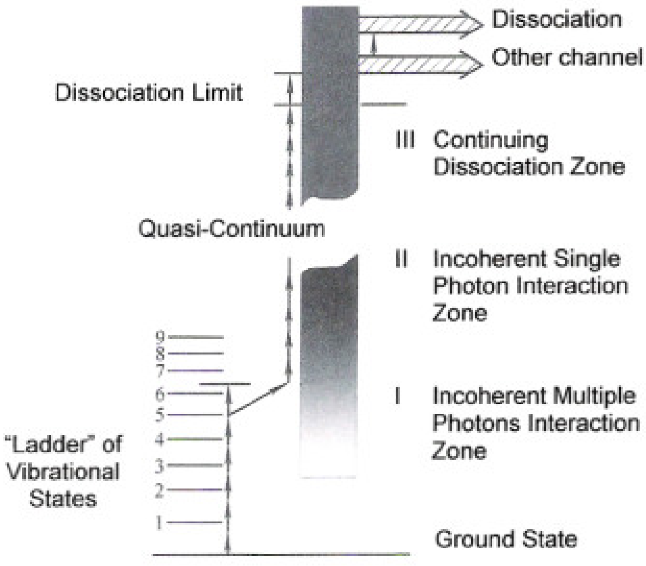

Fig. 1 Molecular level scheme for Infrared Multiphoton Excitation and Dissociation.

METHANE VIBRATIONAL ENERGY LEVELS

To illustrate the complexity of the molecular vibrations caused by IR-excitation, we can use the energy-transfer in methane (CH_4) as an example.

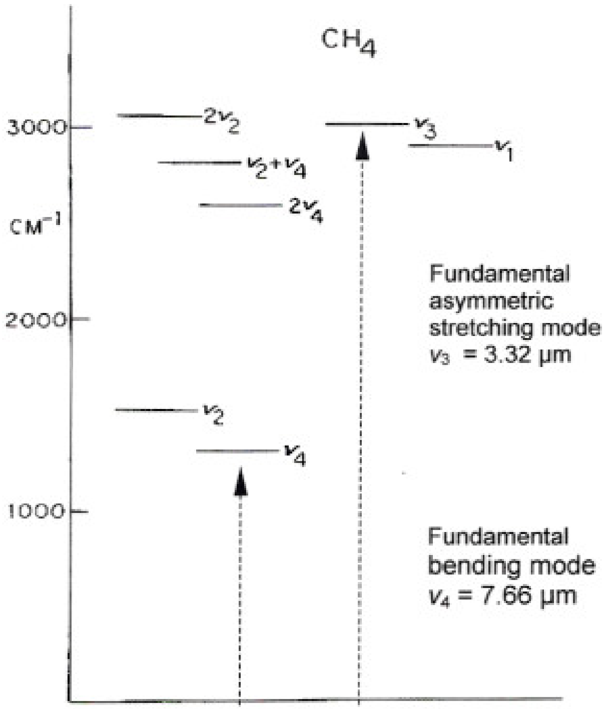

Fig. 2 Partial vibrational energy level diagram of CH_4.

Methane (CH_4) was the first polyatomic molecule for which vibrational energy-transfer pathways and rates were investigated [15]. Single Modes, or fundamental vibration energy levels of methane include asymmetric stretching vibration v_3 at 3010 cm^{-1} (3.32 μm), bending mode v_4 at 1306 cm^{-1} (7.66 μm), and v_1 and v_2, which are the equilibration of v_3 and v_4, respectively. Methane's vibrational energy levels may also include combination modes and overtones such as $2v_4$, $v_2 + v_4$, and $2v_2$. Further equilibration of states is postulated to occur involving more overtones and combination bands, though fully comprehending the system is impossible.

According to Figures 1 and 2, methane molecules absorb a number of IR photons that match its fundamental and/or combination modes to climb up the ladder of vibrational states. As such, IR-excited methane molecules are in excited states where the activation barrier of reaction is lowered as shown in Fig. 3. The activation barrier is the potential energy of reactants required to be overcome in order for the reaction to take place [16]. The height of the activation barrier (or the activation energy required) between reactants and products determines the rate at which the reaction may occur. The lower the activation barrier is, the better the reaction rate will be, as it will take less energy to break up an excited methane molecular structure.

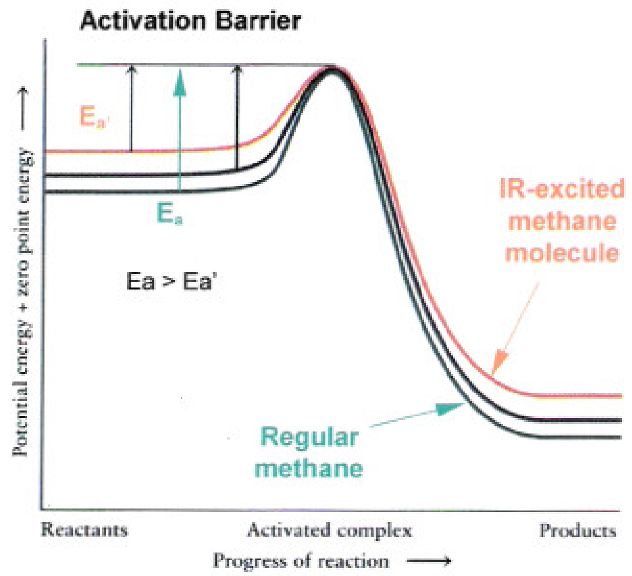

Fig. 3 Reaction profiles of regular and IR-excited methane.

The reaction rate W is determined by Arrhenius equation:

$$W = k\,e^{-E/RT}$$

Where k is a constant, R the universal gas constant, T temperature in ^{o}K, E the activation energy (the energy required to overcome activation barrier). The lower the activation barrier is, the higher the reaction rate will be. As previously stated, in early study of chemical kinetics increasing reaction rate was usually accomplished by raising the reaction temperature T. However, Evans and Polanyi suggested that the increasing reactant vibrational energy (i.e. reducing required activation energy E) is the most effective at promoting reaction. In experiments, increasing reactants vibrational energy was indeed found to enhance the reaction rate more significantly than simply raising the reaction temperature.

FABRICATION OF IR-EMITRERS

Broadband IR-emitters comprised of metal oxides have been broadly used in Japan for agricultural applications since the 1960's. Japanese are particularly successful in using 8 – 20 μm "far-infrared" (but categorized as "mid-infrared" by NASA) in heating and drying agricultural produces for preserve. Prolific experimental data that characterize IR-emitting metal oxides are available in Japan. Based on this known Japanese research, we could tailor IR-emitters using selective transition metal oxides to emit 3 - 14 μm wavelengths.

Transition metal oxide has such a unique property that its constituent electrons can be thermally agitated to reach a neighboring higher energy level; when the excited electron returns to its initial level, it emits IR photons in 3 - 14 μm wavelength range, depending on the variety of oxides used. We had made a 3 - 14 μm IR-emitter for our fuel applications by adding ZrO_2, CoO, and other oxides to $2MgO \cdot 2Al_2O_3 \cdot 5SiO_2$, one of the most popular IR ceramics in Japan [5]. An IR-emitting composite can be made by sintering the mixture of selected oxides powders and bonding agents at above 1300 °C. The resultant ceramic composite continuously absorb ambient heat and emit IR photons in 3 - 14 μm wavelengths. Thus, IR emissions can last indefinitely. In essence, the IR-ceramic is an energy converter that absorbs ambient heat and converts it into IR photons to maintain thermal equilibrium.

An SEM/EDS (scanning electron microscope with energy dispersive spectrometry) plot was run with IR-emitter to obtain a quantitative analysis showing general elemental composition of the oxide compounds. The results are presented in Table 2.

Table 2. Elemental composition of the oxide compounds.

Element	Wt.%	Cmpt.	CmptWt%	Cnts/s	Atomic %
O*	41.12				60.41
Na	0.70	Na_2O	1.18	5.85	0.71
Mg	5.58	MgO	9.25	70.52	5.40
Al	14.19	Al_2O_3	26.80	208.33	12.36
Si	17.73	SiO_2	37.93	261.02	14.84
K	1.35	K_2O	1.62	17.41	0.81
Fe	1.04	Fe_2O_3	1.48	6.69	0.44
Co	1.43	CoO	1.82	7.77	0.57
Zn	1.18	ZnO	1.47	3.67	0.43
Zr	15.69	ZrO	18.44	0.93	4.04

Sample conditions: 20.0 KV; Beam Current (175.0 picoAmps); Tilt Angle (0 deg.); Working Distance (20 mm); TakeOff Angle (35.6°); Solid Angle*BeamCurrent: 1.4.

For the ease of implementation, a partial-tubular shape is designed as shown in Fig. 4, which can easily be tied to the exterior of a non-metal fuel supply line of engines to absorb engine radiation heat and emit infrared.

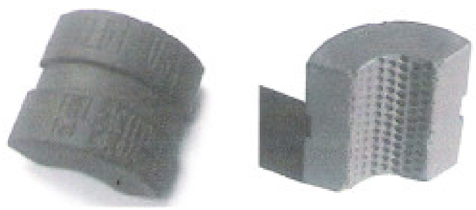

IR-emitter Top View   Bottom View

Fig. 4 Picture of IR-emitter, 1" x 1" x 3/8" in size.

METHANE-AIR COUNTERFLOW EXPERIMENTS

Counterflow flames are widely used in the evaluation of chemical kinetic rates because they are one-dimensional and have a uniform strain rate. The experiments were performed at Purdue's Zucrow Laboratories and the geometry of the burner is similar to the one designed by Puri et al [17] as shown in Fig. 5, with a picture of laminar flame in Fig. 6.

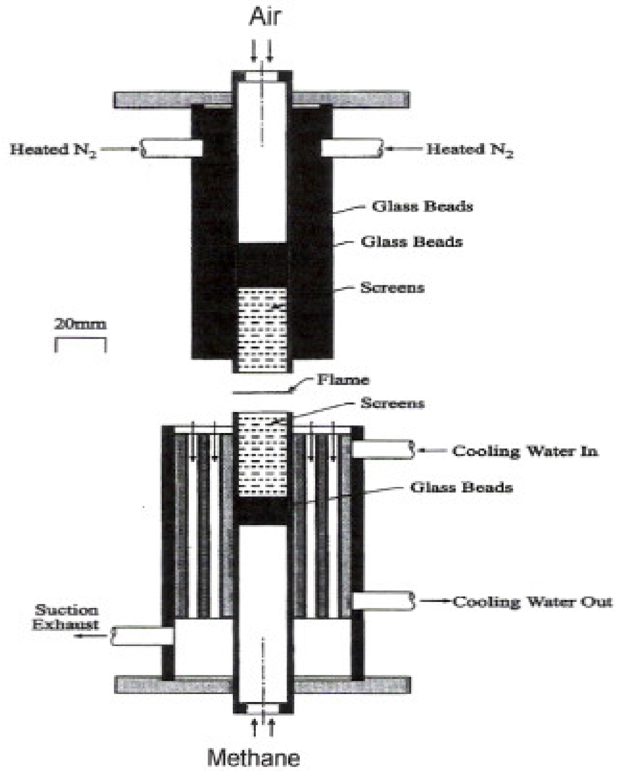

Fig. 5 Schematic of the counterflow burner.

Fig. 6 Opposed-flow flame, flow speed = 25 cm/s.

Numerical Predictions

A detailed description of equations governing conterflow flames is given by Kee et al. [8]. The OPPDIF code was used to predict the flame structure. The energy equation in the code involves variable specific heat, variable thermal conductivity, and variable mass diffusion velocities for the different species and a volumetric energy source term involving all reaction steps. All thermophycal properties were taken from the GRI-Mech 2.11 thermodynamic database [9]. Fig. 7 shows an exemplar of numerical predictions of mole fractions for various species (CH_4, N_2, CO, CO_2 and NO) across the counterflow flame, plotted as a function of distance from the fuel duct, in which the flame locates at where the fuel (CH_4) mole fraction reach its minimum value.

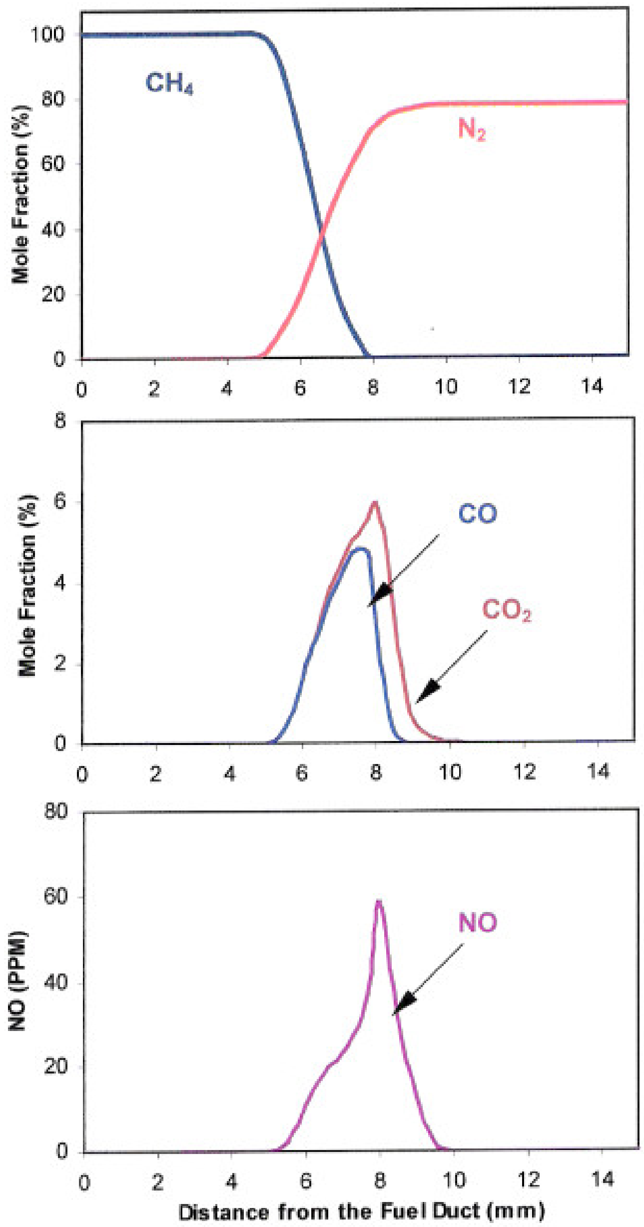

Fig. 7 Numerical predictions of species CH_4, N_2, CO, CO_2, and NO mole fractions across the flame at a flow speed = 25 cm/s.

RESULTS AND DISCUSSION

The experiments were performed with methane (Airco Gas and Gear, 99% methane) introduced from the bottom duct and air from the top duct. A nitrogen coflow was introduced from the top duct to stabilize the flames. The separation distance between the two ducts is 15 mm and the inner diameter of both ducts is 20 mm. The velocity is 10 cm/sec, calculated assuming uniform flow at the exit. In order to verify the effect of infrared excitation on the fuel, a control valve, as shown in Fig. 8, was used to selectively direct the fuel through either a regular Teflon line (for Baseline measurements) or the line with IR-emitters attached to it (for IR-excited measurements).

Measurements of mole fraction of gas species were made using a quartz microprobe, which had an outer diameter of 2.97 mm and a conical tip reducing the frontal outer diameter to 0.5 mm over a distance of 10 mm. The inner diameter was 0.080 mm. Gas samples along the line of symmetry were withdrawn at various axial distances from the fuel tube by positioning the probe at a radial distance of 1 mm near the axis. Species distributions in the flame were measured by using a gas chromatograph (GC) (Shimadzu, GC8A). The nitric oxide (NO) distribution was measured using a calibrated chemiluminescence analyzer (Thermo Environmental Instruments, 42H).

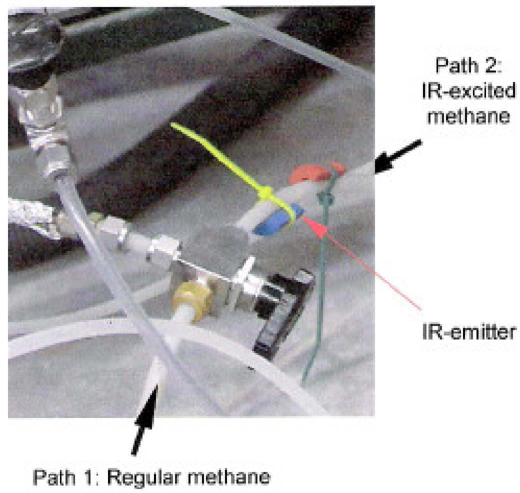

Fig. 8 Controllable feeding paths for methane.

Measured N_2 and CH_4 Distributions

Fig. 9 shows measured mole fractions of N_2 and CH_4, plotted as a function of distance from an approximate center between the fuel duct and the air duct, both ducts being separated at a distance of 15 mm. The data show that the flame location where the fuel CH_4 mole fraction reaches its minimum value moves toward the fuel duct because the momentum of the fuel stream decreases with IR-excitation at a constant velocity. The plotted curves of measured N_2 and CH_4 mole fractions of IR-excited fuel moving toward the fuel duct indicates that diffusion flame occurs earlier, meaning IR-excited fuel combusts faster than regular fuel.

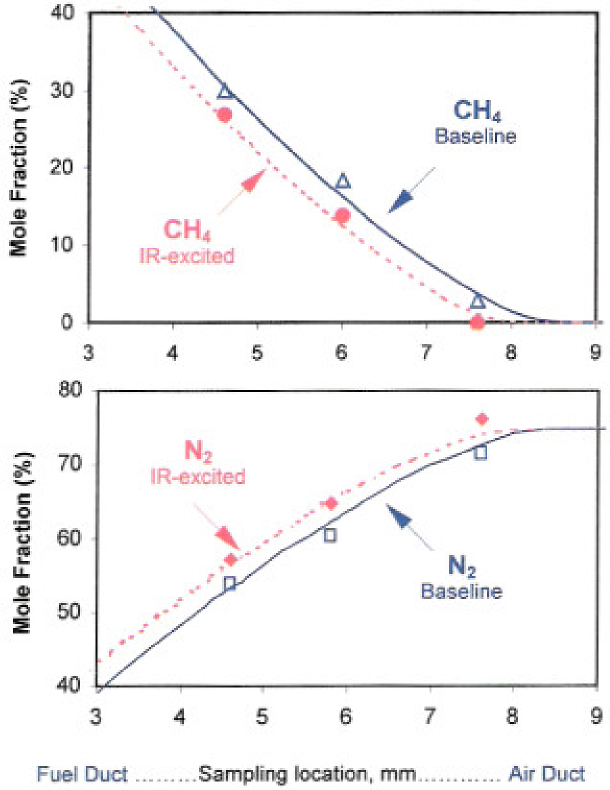

Fig. 9 Measurements of N_2 and CH_4 mole fractions.

The lines associated with measured data points shown in Fig. 9 are computational predictions made by using OPPDIF code.

Meanwhile, the fuel consumption rate can be calculated by integrating the net volumetric consumption rate over the entire computational domain [18]:

$$Fuel\ Consumption\ Rate = \int_0^L \varpi_{CH4}\, dx$$

where L is the distance between the ducts and ω_{CH4} is the volumetric consumption rate in moles/cm^3/sec. Based on the measurements of CH_4 mole fractions, the Fuel Consumption Rate of IR-excited methane is calculated to be 6 % less than that of regular methane.

Measured CO and CO_2 Distributions

Fig. 10 displays the measured mole fractions of carbon monoxide (CO) and carbon dioxide (CO_2) respectively for regular methane and IR-excited methane. The data show the peak CO emissions of IR-excited methane are about 25% less, compared to regular methane. Due to a faster combustion as indicated in CH_4 measurements, the fuel consumption rate is decreased that resulted in less CO_2 and CO being produced in combustion process, where CO is a precursor of CO_2.

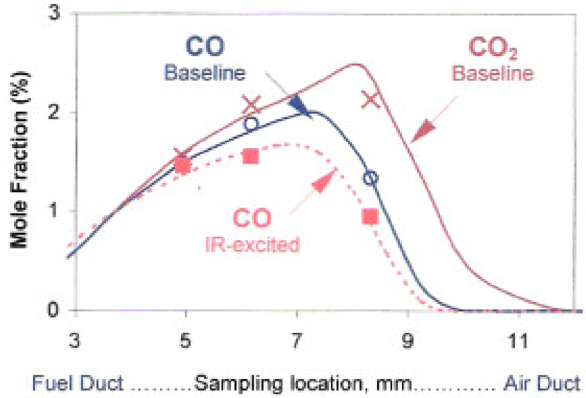

Fig. 10 Measurements of CO and CO_2 mole fractions.

Measured Nitric Oxide (NO) Distributions

The measurements of nitric oxide (NO) emissions are plotted in Fig. 11 for comparisons between IR-excited methane with regular methane. The data show not only a lower peak NO emission with IR-excited methane, but also a smaller area under the curve of NO measurements, indicating less total NO emissions produced during the combustion. Thermal NO formation is always slower than fuel combustion. With a faster combustion, there was less time for NO to form, thus resulting in less NO emissions.

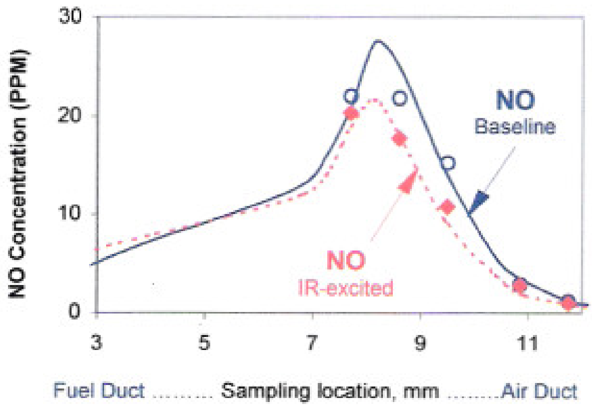

Fig. 11 Measurements of NO emissions.

The ***EIJ***, emission index for species *J* (in this case *J* = NO), is calculated following Takeno and Nishika [18]:

$$EIJ = \frac{\int_0^L M_J \varpi_J\, dx}{\int_0^L M_{CH4} \varpi_{CH4}\, dx}$$

where M_J is the molecular weight of species *J* and ω_J is the volumetric production rate of species *J* in moles/cm^3/s. The EI_{NO}, emission index for NO in combustion of IR-excited methane is computed to be about 15% less than regular methane.

ENGINE-STAND TESTS AT PURDUE

Tests on a GM Quad-4 Gasoline Engine

IR-emitter was installed on a 2000 GM Quad-4 2.4 L gasoline engine at Purdue Engine Labs to demonstrate its effect on the Specific Fuel Consumption (SFC) rates of the engine. The tests were run at variable speeds under a constant load of 20 ft-lb and the data are listed and plotted in Fig. 12, as a function of engine speed RPMs. An average improvement of 6% in fuel consumption over the test speeds range is observed with IR-emitter installed.

Speed RPM	SFC-Baseline	SFC-w/FIR	Improvement
1800	0.8369	0.7839	- 6.76%
2200	0.8381	0.7852	- 6.74%
3000	0.8072	0.7693	- 4.93%

(SFC unit: lb/hp-hr)

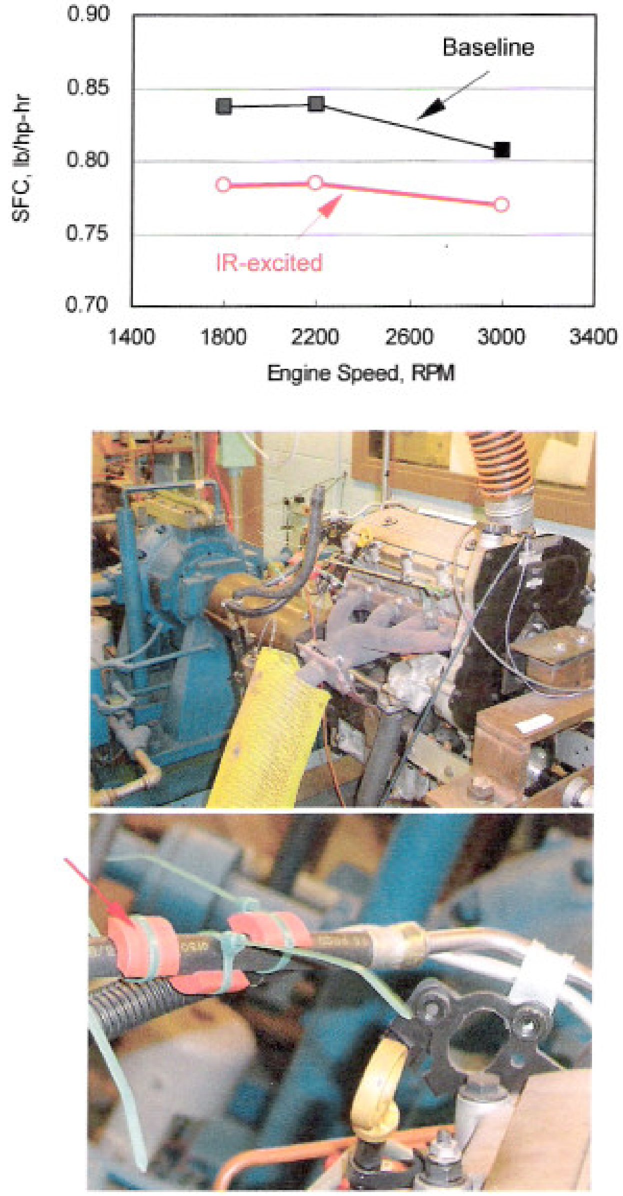

Fig. 12 SFC measurements on a GM Quad-4 engine.

Emissions on a Single-cylinder Engine

IR-emitter was tested at Engine Lab of Purdue University on a PowerTek Single-Cylinder Engine/Dynamometer, as shown in Fig. 13. The engine displacement is 213 cc with a rated maximum power of 5.6 kW. The test was performed at various engine speeds (1000, 1500 and 2000 rpms) under a 40% constant load. Propane fuel was used to verify IR-effect on reducing CO and NOx emissions. The data were automatically collected and are displayed in Table 4, which show an average 14.5 % reduction in CO and 10.2 % reduction in NOx emissions, respectively.

Table 4. CO & NOx Emissions test with propane fuel

	CO (ppm)			NOx (ppm)		
RPM	**1500**	**2000**	**2500**	**1500**	**2000**	**2500**
Baseline	542	1051	1596	254	95	37
R-emitter	468	820	1472	247	79	33
Change %	-13.7	-22.0	- 7.8	- 2.8	- 16.8	- 10.8

Fig. 13 PowerTrek single cylinder dynomometer.

BETA-SITE VHEICLE TESTS

Emissions on a Chinese Iveco Diesel Engine

IR-emitter was tested at Shanghai Vehicle Performance Testing Center (Shanghai, China) on a light-duty pickup shown in Fig. 14, which has a 4-cyl. 2.8 L diesel engine with a rated 87 kW maximum power, made in 1997 by Iveco-China. The tests were performed following standard Chinese testing protocols. The vehicle ran on a dynomometer at variable speeds with a preset 60 N.m load. The results on NOx and smoke emissions are listed in Table 3. It seen that both NOx and smoke emissions are simultaneously reduced, which might seem counter-intuitive, becuase it is generally belived that a tradeoff between NOx and smoke exists. Nevertheless, the simultaneous reduction in both pollutants can be explained by the results from aforementioned methane-air counterflow flame experiments.

Table 3 Test results on Iveco light-duty diesel engine.

(a) NOx Emissions, ppm

Speed, km/h	30	40	50	60	Avg.
Baseline	642	567	505	431	
w/ IR-Emitter	598	530	463	410	
Change	-6.8%	-6.5%	-8.3%	-4.6%	-6.6%

(b) Smoke Emissions, % Opacity

Speed, km/h	30	40	50	60	Avg.
Baseline	16.6	15.8	10.6	6.6	
w/ IR-Emitter	12.4	11.2	7.3	6.0	
Change	-25.3%	-29.1%	-31.1%	-9.1%	-23.7%

Fig. 14 An Iveco diesel pickup tested by the Shanghai Vehicle Performance Testing Center.

Improved Performance of Diesel School Bus

Beta-site tests were also conducted on school buses at a community school district of Greenwood, Indiana. The test bus was a 2004 International CE School Bus, having a modern International VT365 V-8 6.0 L diesel engine with EVRT technology, shown in Fig.15. It ran a regular 60-mile route each school day. The driver carried a fuel card, with which the number of gallons of diesel re-fueled was automatically recorded with the odometer-mileage and data sent directly to fleet supervisor's computer for filing.

Fig. 15 An International School Bus with IR-emitter.

The graph in Fig.16 was generated by using the recorded fueling data. The Baseline fuel economy was computed to be 5.67 miles per gallon (MPG), based on the fueling records over nearly a year from 9/1/04 thru 10/14/05. IR-emitter was installed on 10/14/05 and data were collected for ensuing six months, 10/14/05 – 5/8/06. The average fuel economy with IR-emitter is computed to be 6.23 MPG. Later, IR-emitter was removed on 5/8/06 and the average fuel economy decreased to 5.41 MPG, near its previous baseline. The improvement on fuel economy by using IR-emitter is calculated to be about 12%.

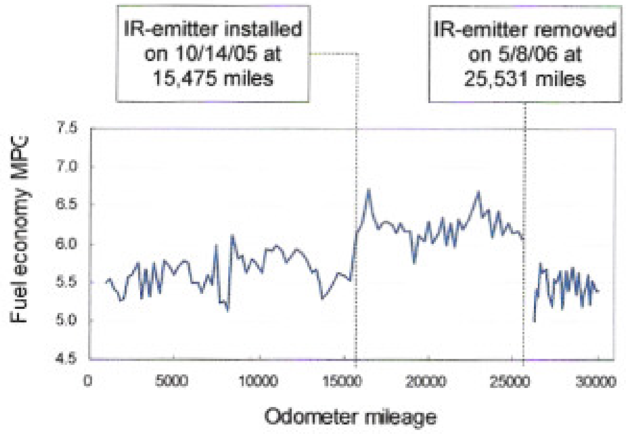

Fig. 16 Refueling records on an International School Bus.

SUMMARY AND CONCLUSIONS

We have developed an innovative technology using 3 – 14 μm wavelength mid-infrared to excite hydrocarbon fuels for increased combustion efficiency in internal combustion engines. IR-emitter can be made from selective transition metal oxides by sintering the mixture of powders and bonding agents at 1300°C. When retrofitted to the exterior of a nonmetal supply fuel line of an engine, the IR-emitter absorbs radiation heat from the engine and emits IR photons in 3 – 14 μm wavelengths. IR photons in this wavelength range can penetrate nonmetal fuel hose and excite the fuel traversing through the fuel line.

The HC molecule in fuel absorbs a number of IR-photons at assorted wavelengths, known as molecular multiphoton process (MMP), causing molecular vibrations. Excited hydrocarbon's constituent electrons can climb up the ladder of vibrational states and reach excited states. IR-excited fuel has lowered activation barrier for reaction with increased combustibility to burn faster in cylinders, allowing more heat released from the fuel in early cycle to do mechanical work and less in later cycle as heat loss to raise exhaust gas temperature (EGT).

In essence, the IR-emitter works as an energy converter that absorbs radiation heat from the engine and emits IR photons. These photons are used to excite hydrocarbons and promote heat release in earlier cycle, allocating more heat to do work and less heat to raise EGT. This results in increased power, lower specific fuel combustion and reduced HC, CO, NOx, and CO_2 emissions.

Based on the preliminary lab investigations and beta-site engine and vehicle tests, conclusions of the present study can be made as follows:

1. IR-excitation causes the counter-flow methane-air to combust faster, resulting in reduced fuel consumption and decreased CO and NO emissions.
2. Hydrocarbons are infrared-active so that IR-excitation will work on all HC-based fuels, including natural gas (methane), propane, gasoline, diesels and bio-diesels.
3. IR-excitation helps reduce Specific Fuel Consumption and all targeted emissions such as HC, CO, NOx, and CO_2 from gasoline or diesel engines.

Though the present study has demonstrated IR-excitation effect is factual in various tests, how it participates in the thermochemical process of combustion remains to be experimentally studied. The IR-excited fuel technology provides a fuel-pretreatment means for increasing combustion efficiency of gasoline and diesel engines. It can be retrofitted on nearly all old or new production engines that are currently in use without changing the engine specifications. Yet, how IR-excited fuel actually improves gasoline and diesel engine performance needs be experimentally examined in details before a conclusion can be made. Future research on optimizing IR-emitting composition is also required.

ACKNOWLEDGMENTS

The authors wish to thank Professor Joseph F. Kmec and his students at Engine Laboratories, Dept. of Mechanical Engineering Technology, Purdue University, for testing IR-device on GM Quad-4 gasoline engine, and Professor Sara E. Leach, Dept. MET, Purdue University, for compositional analysis on IR-emitter. Thanks extended to fleet personnel at the Greenwood Community Schools District and Heritage Transport for voluntarily participating in the beta-site school bus and truck tests. Last, but not least, sincere thank to Mr. Paul D. Davis, Group Transportation Manager, Nestlé U.S.A., for his kind support and valuable leadership in implementing the fleet testing program.

CONTACTS

Albert C. Wey, Inventor of the IR-Excited Fuel technology; B.S. in Electrophysics from Taiwan Chiao-Tung University (1977), Ph.D. (1985) degrees in Electrical Engineering from the State University of New York at Stony Brook; MBA degree from the University of Chicago (1994); e-mail: wey.albert@yahoo.com Phone: (630) 632-1415.

Rodney G. Handy, Associate Professor, Department of Mechanical Engineering Technology, Purdue University, e-mail: rhandy@purdue.edu

Yuan Zheng, Research Assistant Professor, Maurice J. Zucrow Laboratories, School of Mechanical Engineering, Purdue University, e-mail: zhengy@ecn.purdue.edu

REFERENCES

1. Wey A, "Effect of Infrared-Irradiated Fuels on Smoke Reduction of A Diesel Engine – An Initial Study", Proceedings of AFS Fall 2003 Topical Conference, 9/30 – 10/2. Ann Arbor, MI.
2. Smith M, "Organic Chemistry", Harper Collins Publisher, New York (1993), p. 413.
3. Turro N J, "Modern Molecular Photochemistry", Benjamin-Cummins, Menlo Park, 1978.
4. Chiu T. H., "The Principle and Application of Far-Infrared Heating", 1995, Wen-Seng Publisher, Taiwan, p. 31 – 45.
5. Wey A, "Infrared-Irradiated Fuels for Increased Fuel Conversion Efficiency", Proceedings of AFS Fall 2005 Topical Conference, 9/19 – 22. Ann Arbor, MI.
6. Lim J., Gore J., and Viskanta R., "A Study of the Effects of Air Preheat on the Structure of Methane/Air Counterflow Diffusion Flames", Combustion and Flame 121, p. 262 – 274 (2000)
7. Lutz A. E., Kee R. J., Grear J. F., and Ruply F. M., Sandia Report SAND96-8243 (1996).
8. Kee R. J., Miller J. A., Evans J. H., and Dixon-Lewis G., 22nd Symposium (International) on Combustion, p. 1479 – 1495 (1988).
9. Bowman C. T., Hanson R. K., Davidson D. F., Gardiner Jr. W. C., Lissianski V., Smith G. P., Golden D. M., Frenklach M., and Goldenberg M., http://www.me.berkeley.edu/gri_mech. GRI-Mech 2.11 (1996)
10. Chemical Physics Handbook, "Infrared Correlation Chart," p. 9-87 – 9-89 (2004)
11. Evans M. G. and Polanyi M., Trans. Faraday Soc., 35, P. 178 (1939)
12. Karny Z. and Zare R. N., J. Chem. Phys., 68, 3360 (1978)
13. Reiser C, MIT Ph.D. Thesis, "Mechanism of Multiple Infrared Photon Absorption and Dissociation" (1980).
14. Mukamel S. "Reduced Equations of Motion for Collisionless Molecular Multiphoton Process", Photoselective Chemistry, Adv. Chem. Phys., vol. 47 (1981) p. 509.
15. Weitz E and Flynn G, "Vibrational Energy Flow in the Ground Electronic States of Polyatomic Molecules", Photoselective Chemistry, Adv. Chem. Phys., vol. 47 (1981) p. 185.
16. Atkins P.W., "Quanta", Oxford University Press, New York, 1991, P. 101
17. Puri I. K., Seshadri K., Smooke M. D., and Keys D. E., Combustion Science Technology, vol. 56, p. 1 – 12 (1987).
18. Takeno T., and Nishioka M., Combustion Flame 92, p. 465 – 468 (1993).

ATTACHMENT B

Sygma Test Fleet Trailers

WORLDKLASS TECHNOLOGIES
SYGMA NETWORK TRAILER NUMBERS
OKLAHOMA CITY: JULY 2015 - FEBRUARY 2017
PREPARED: 01MAR2018 / UPDATED: 16MAR2018

	TEST GROUP (WITH TECHNOLOGY CANISTERS)		CONTROL GROUP (NO TECHNOLOGY CANISTERS)
COUNT	TRAILER NUMBER	DATE OF CANISTER INSTALLATION	TRAILER NUMBER
1	242257	25-Jul-15	242256
2	216660	25-Jul-15	216652
3	216661	21-Aug-15	216654
4	216669	21-Aug-15	216655
5	216674	21-Aug-15	216656
6	216675	25-Jul-15	216657
7	216676	21-Aug-15	216658
8	216677	21-Aug-15	216659
9	216679	25-Jul-15	216662
10	216681	25-Jul-15	216663
11	217022	21-Aug-15	216664
12	217023	21-Aug-15	216665
13	217024	25-Jul-15	216666
14	217025	21-Aug-15	216667
15	217026	25-Jul-15	216668
16	217374	21-Aug-15	216670
17	219486	21-Aug-15	216671
18	219488	25-Jul-15	216672
19	219502	25-Jul-15	216673
20	219516	21-Aug-15	216678
21	239847	25-Jul-15	216680
22			216682
23			217335
24			217372
25			217378
26			228730
27			219489
28			219507
29			219515
30			219532

Note 1: Control Group previously included Trailers whose numbers ended in 2524, 6647, 6648, and 7364. These trailers subsequently excluded because of they were Out-Of-Service for a significant portion of the field trial duration.

ATTACHMENT C

Sygma Engine Hours Data Capture Card (Representative Sample)

TRAILER HOURS - PERIOD 1-18										
216654	49622	46836	46888	46930	46950	46995	47023	47070	47085	47129
216655	49624	35579	35636	35664	35726	35775	35850			
216656	49626	40233	40286	40303	40354	40413	40474	40508	40546	
216657	49628	30338	30356	30390	30401	30436	30513			
216658	49630	33307	33338	33357	33382	33441	33471	33482	33536	33558
216659	49652	34315								
216660	49654	32262								
216662	49658	34311	34369	34411	34446	34529	34584	34630	34651	34772
216663	49660	32550	32591	32629	32664	32723	32772	32822	32870	32910
216664	49682	38249								
216665	49684	37403	37420	37456	37483	37527	37575	37630	37665	37702
216668		33115	33132	33148	33164	33185	33204	33230	33256	33274
216669	49712	33997								
216670	49714	30673								
216671	49716	33334	33390	33413	33442	33481	33505	33546	33594	33617
216672	49718	32316	32361	32373	32439	32509	32550	32564	32598	32632
216673	49720	33146	33197	33240	33272	33314	33341	33452		
216674	49742	31593	31599	31656	31689	31724	31775	31816	31857	31914
216675	49744	5610								
216676	49746	31784	31839	31874	31915	31960	32013	32044	32120	
216677	49748	28113	28122	28188	28247	28284	28308	28350	28396	28448
216678	49750	30217	30250	30266	30362-	?30399	30448	30491	30530	30569
216679	49782	16722	16851	16879	16890	16959	~~17~~17033			
216680	49784	23250	23289	23319	19728-	?19784	19807			
216681	49786	21458	21537	21575	21638	21684	21733	21776	21834	21861
216682	49788	23020	23055	23101	23513-	?23214	23274	23331		
217022	50008	31715	31735	31750	31780	31827	31829	31864	31874	31913
217023	50010	45421								
217024	50032	354	394	427	466	503	548	638	670	769
217025	50034	22590	22661	22730	22777	22830	22883	22922		
217026	50036	23515	23542	23582	23624	23674	23705	23747	23787	23842
217335	51074	29581	29592	29630	29690	29713	29766	29794	29822	29841
217364	51094	33363								
217372	51124	5963	5988	6038	6054	6082				
217374	51126	33345	33370	33415	33473	33523	33576	33635	33716	33764
217378	51144	35541	35572	35604	35681	35738	35789	35834	35876	35935
219486	49221	17934	17985	18007	18081	18156	18174	18236	18296	18337
219488	49223	18845	18872	18886	18943	18974	18996	19043	19083	19123
219489	49225	21049	21104	21137	21192	21249	21303	21330	21377	21415
219507	49257	19131	19163	19228	19257	19282	19309			
219515	49287	18139	18150	18236	18257	18280	18349	18401	18466	18498
219516	49289	17799	17831	17855	17880	17900	17936	17954	17999	18001
219532	49317	18896	18924	18953	18986	19020	19056	19097	19120	19219
228730	49665	15044	15071	15112	15169	15194	15223	15250	15291	15352
239847	50089	8779	8818	8832	8836	8870	8896	8939	8983	
242256	50199	19393	19457	19511	19545	19561	19602	19647	19688	19751
242257	50211	18906	18945	18969	18998	19005	19092	19136	19155	19184
243787	63296	5610	5655	5686	5695	5746	5847	5884		
243793	63298	5657	5699	5724	5819	5858				
244419	65532	5347	5379	5428	5436	5491	5545	5579	5643	5668
244457	65960	5325	5365	5427	5454	5507	5537	5582	5602	5645
244494	65666	4804	4870	4913	4957	4983	5013	5070	5122	5162

244498	65962	4757	4797	4845	4939	4942	4989	5004	5022	5058
245199		1070	1076	1108	1139	1195	1227	1264	1300	1343
245200		1063	1122	1166	1264	1328	1367			
245202		1666	1724	1764	1789	1839	1879	1931	1956	1975
245206		954	985	1009	1048	1097	1116	1120	1153	
245211		1056	1111	1148	1163	1197	1240	1302	1327	1359
245323		1767	1806	1826	1856	1903	1951	1989		
245338		1641	1715	1716	1777	1783	1826	1871	1945	1970

216654										
216655										
216656										
216657										
216658	33577	33601								
216659										
216660										
216662	34811									
216663										
216664										
216665	37738	37762								
216668	33293									
216669										
216670										
216671	33663	33711								
216672										
216673										
216674										
216675										
216676										
216677										
216678										
216679										
216680										
216681										
216682										
217022	31996	32046								
217023										
217024										
217025										
217026										
217335	29903									
217364										
217372										
217374										
217378	35947	35974								
219486										
219488	19148									
219489	21430									
219507	19343									
219515										
219516	18053									
219532										
228730	15366	15402								
239847										
242256	10808									
242257										
243787										
243793										
244419										
244457										
244494										

244498	5095									
245199	1411	1452								
245200										
245202	2015	2021	2059							
245206										
245211	1396									
245323										
245338										

ATTACHMENT D

Sysco / Sygma Fiscal Calendars (2015, 2016 and 2017)

2015 FISCAL YEAR CALENDAR - June 29, 2014 to June 27, 2015

Sysco Corporation

07/27/18 11:36 AM

FIRST PERIOD
June 29th - July 26th

S	M	T	W	T	F	S	wk#
29	30	1	2	3	4	5	**1**
6	7	8	9	10	11	12	**2**
13	14	15	16	17	18	19	**3**
20	21	22	23	24	25	26	**4**

SECOND PERIOD
July 27th - August 23rd

S	M	T	W	T	F	S	wk#
27	28	29	30	31	1	2	**5**
3	4	5	6	7	8	9	**6**
10	11	12	13	14	15	16	**7**
17	18	19	20	21	22	23	**8**

THIRD PERIOD
August 24th - September 27th

S	M	T	W	T	F	S	wk#
24	25	26	27	28	29	30	**9**
31	1	2	3	4	5	6	**10**
7	8	9	10	11	12	13	**11**
14	15	16	17	18	19	20	**12**
21	22	23	24	25	26	27	**13**

FOURTH PERIOD
September 28th - October 25th

S	M	T	W	T	F	S	wk#
28	29	30	1	2	3	4	**14**
5	6	7	8	9	10	11	**15**
12	13	14	15	16	17	18	**16**
19	20	21	22	23	24	25	**17**

FIFTH PERIOD
October 26th - November 22nd

S	M	T	W	T	F	S	wk#
26	27	28	29	30	31	1	**18**
2	3	4	5	6	7	8	**19**
9	10	11	12	13	14	15	**20**
16	17	18	19	20	21	22	**21**

SIXTH PERIOD
November 23rd - December 27th

S	M	T	W	T	F	S	wk#
23	24	25	26	27	28	29	**22**
30	1	2	3	4	5	6	**23**
7	8	9	10	11	12	13	**24**
14	15	16	17	18	19	20	**25**
21	22	23	24	25	26	27	**26**

SEVENTH PERIOD
December 28th - January 24th

S	M	T	W	T	F	S	wk#
28	29	30	31	1	2	3	**27**
4	5	6	7	8	9	10	**28**
11	12	13	14	15	16	17	**29**
18	19	20	21	22	23	24	**30**

EIGHTH PERIOD
January 25th - February 21st

S	M	T	W	T	F	S	wk#
25	26	27	28	29	30	31	**31**
1	2	3	4	5	6	7	**32**
8	9	10	11	12	13	14	**33**
15	16	17	18	19	20	21	**34**

NINTH PERIOD
February 22nd - March 28th

S	M	T	W	T	F	S	wk#
22	23	24	25	26	27	28	**35**
1	2	3	4	5	6	7	**36**
8	9	10	11	12	13	14	**37**
15	16	17	18	19	20	21	**38**
22	23	24	25	26	27	28	**39**

TENTH PERIOD
March 29th - April 25th

S	M	T	W	T	F	S	wk#
29	30	31	1	2	3	4	**40**
5	6	7	8	9	10	11	**41**
12	13	14	15	16	17	18	**42**
19	20	21	22	23	24	25	**43**

ELEVENTH PERIOD
April 26th - May 23rd

S	M	T	W	T	F	S	wk#
26	27	28	29	30	1	2	**44**
3	4	5	6	7	8	9	**45**
10	11	12	13	14	15	16	**46**
17	18	19	20	21	22	23	**47**

TWELFTH PERIOD
May 24th - June 27th

S	M	T	W	T	F	S	WK
24	25	26	27	28	29	30	**48**
31	1	2	3	4	5	6	**49**
7	8	9	10	11	12	13	**50**
14	15	16	17	18	19	20	**51**
21	22	23	24	25	26	27	**52**
28	29	30	1	2	3	4	**1**
5	6	7	8	9	10	11	**2**

US Holidays (highlighted dates: July 4, September 1, November 27, November 28, December 25, December 26, January 1, May 25, July 3)

2016 FISCAL YEAR CALENDAR - June 28, 2015 to July 2, 2016 **The SYGMA Network**

FY 2016

FIRST PERIOD *June 28th - July 25th*							**P1**
S	**M**	**T**	**W**	**T**	**F**	**S**	**wk#**
28	29	30	1	2	3	4	**1**
5	6	7	8	9	10	11	**2**
12	13	14	15	16	17	18	**3**
19	20	21	22	23	24	25	**4**

SECOND PERIOD *July 26th - August 22nd*							**P2**
S	**M**	**T**	**W**	**T**	**F**	**S**	**wk#**
26	27	28	29	30	31	1	**5**
2	3	4	5	6	7	8	**6**
9	10	11	12	13	14	15	**7**
16	17	18	19	20	21	22	**8**

THIRD PERIOD *August 23rd - September 26th*							**P3**
S	**M**	**T**	**W**	**T**	**F**	**S**	**wk#**
23	24	25	26	27	28	29	**9**
30	31	1	2	3	4	5	**10**
6	7	8	9	10	11	12	**11**
13	14	15	16	17	18	19	**12**
20	21	22	23	24	25	26	**13**

FOURTH PERIOD *September 27th - October 24th*							**P4**
S	**M**	**T**	**W**	**T**	**F**	**S**	**wk#**
27	28	29	30	1	2	3	**14**
4	5	6	7	8	9	10	**15**
11	12	13	14	15	16	17	**16**
18	19	20	21	22	23	24	**17**

FIFTH PERIOD *October 25th - November 21st*							**P5**
S	**M**	**T**	**W**	**T**	**F**	**S**	**wk#**
25	26	27	28	29	30	31	**18**
1	2	3	4	5	6	7	**19**
8	9	10	11	12	13	14	**20**
15	16	17	18	19	20	21	**21**

SIXTH PERIOD *November 22nd - December 26th*							**P6**
S	**M**	**T**	**W**	**T**	**F**	**S**	**wk#**
22	23	24	25	26	27	28	**22**
29	30	1	2	3	4	5	**23**
6	7	8	9	10	11	12	**24**
13	14	15	16	17	18	19	**25**
20	21	22	23	24	25	26	**26**

SEVENTH PERIOD *December 27th - January 23rd*							**P7**
S	**M**	**T**	**W**	**T**	**F**	**S**	**wk#**
27	28	29	30	31	1	2	**27**
3	4	5	6	7	8	9	**28**
10	11	12	13	14	15	16	**29**
17	18	19	20	21	22	23	**30**

EIGHTH PERIOD *January 24th - February 20th*							**P8**
S	**M**	**T**	**W**	**T**	**F**	**S**	**wk#**
24	25	26	27	28	29	30	**31**
31	1	2	3	4	5	6	**32**
7	8	9	10	11	12	13	**33**
14	15	16	17	18	19	20	**34**

NINTH PERIOD *February 21st - March 26th*							**P9**
S	**M**	**T**	**W**	**T**	**F**	**S**	**wk#**
21	22	23	24	25	26	27	**35**
28	29	1	2	3	4	5	**36**
6	7	8	9	10	11	12	**37**
13	14	15	16	17	18	19	**38**
20	21	22	23	24	25	26	**39**

TENTH PERIOD *March 27th - April 23rd*							**P10**
S	**M**	**T**	**W**	**T**	**F**	**S**	**wk#**
27	28	29	30	31	1	2	**40**
3	4	5	6	7	8	9	**41**
10	11	12	13	14	15	16	**42**
17	18	19	20	21	22	23	**43**

ELEVENTH PERIOD *April 24th - May 21st*							**P11**
S	**M**	**T**	**W**	**T**	**F**	**S**	**wk#**
24	25	26	27	28	29	30	**44**
1	2	3	4	5	6	7	**45**
8	9	10	11	12	13	14	**46**
15	16	17	18	19	20	21	**47**

TWELFTH PERIOD *May 22nd - July 2nd*							**P12**
S	**M**	**T**	**W**	**T**	**F**	**S**	**wk#**
22	23	24	25	26	27	28	**48**
29	30	31	1	2	3	4	**49**
5	6	7	8	9	10	11	**50**
12	13	14	15	16	17	18	**51**
19	20	21	22	23	24	25	**52**
26	27	28	29	30	1	2	**53**

US Holidays

2017 FISCAL YEAR CALENDAR - July 3, 2016 to July 1, 2017 **Sysco Corporation**

FIRST PERIOD
July 3rd - July 30th

S	M	T	W	T	F	S	wk#
3	4	5	6	7	8	9	**1**
10	11	12	13	14	15	16	**2**
17	18	19	20	21	22	23	**3**
24	25	26	27	28	29	30	**4**

SECOND PERIOD
July 31st - August 27th

S	M	T	W	T	F	S	wk#
31	1	2	3	4	5	6	**5**
7	8	9	10	11	12	13	**6**
14	15	16	17	18	19	20	**7**
21	22	23	24	25	26	27	**8**

THIRD PERIOD
August 28th - October 1st

S	M	T	W	T	F	S	wk#
28	29	30	31	1	2	3	**9**
4	5	6	7	8	9	10	**10**
11	12	13	14	15	16	17	**11**
18	19	20	21	22	23	24	**12**
25	26	27	28	29	30	1	**13**

FOURTH PERIOD
October 2nd - October 29th

S	M	T	W	T	F	S	wk#
2	3	4	5	6	7	8	**14**
9	10	11	12	13	14	15	**15**
16	17	18	19	20	21	22	**16**
23	24	25	26	27	28	29	**17**

FIFTH PERIOD
October 30th - November 26th

S	M	T	W	T	F	S	wk#
30	31	1	2	3	4	5	**18**
6	7	8	9	10	11	12	**19**
13	14	15	16	17	18	19	**20**
20	21	22	23	24	25	26	**21**

SIXTH PERIOD
November 27th - December 31st

S	M	T	W	T	F	S	wk#
27	28	29	30	1	2	3	**22**
4	5	6	7	8	9	10	**23**
11	12	13	14	15	16	17	**24**
18	19	20	21	22	23	24	**25**
25	26	27	28	29	30	31	**26**

SEVENTH PERIOD
January 1st - January 28th

S	M	T	W	T	F	S	wk#
1	2	3	4	5	6	7	**27**
8	9	10	11	12	13	14	**28**
15	16	17	18	19	20	21	**29**
22	23	24	25	26	27	28	**30**

EIGHTH PERIOD
January 29th - February 25th

S	M	T	W	T	F	S	wk#
29	30	31	1	2	3	4	**31**
5	6	7	8	9	10	11	**32**
12	13	14	15	16	17	18	**33**
19	20	21	22	23	24	25	**34**

NINTH PERIOD
February 26th - April 1st

S	M	T	W	T	F	S	wk#
26	27	28	1	2	3	4	**35**
5	6	7	8	9	10	11	**36**
12	13	14	15	16	17	18	**37**
19	20	21	22	23	24	25	**38**
26	27	28	29	30	31	1	**39**

TENTH PERIOD
April 2nd - April 29th

S	M	T	W	T	F	S	wk#
2	3	4	5	6	7	8	**40**
9	10	11	12	13	14	15	**41**
16	17	18	19	20	21	22	**42**
23	24	25	26	27	28	29	**43**

ELEVENTH PERIOD
April 30th - May 27th

S	M	T	W	T	F	S	wk#
30	1	2	3	4	5	6	**44**
7	8	9	10	11	12	13	**45**
14	15	16	17	18	19	20	**46**
21	22	23	24	25	26	27	**47**

TWELFTH PERIOD
May 28th - July 1st

S	M	T	W	T	F	S	WK
28	29	30	31	1	2	3	**48**
4	5	6	7	8	9	10	**49**
11	12	13	14	15	16	17	**50**
18	19	20	21	22	23	24	**51**
25	26	27	28	29	30	1	**52**

US Holidays

ATTACHMENT E

Sygma Oklahoma Test Data (P15-1 Through P17-2)

SYGMA REFRIGERATED TRAILERS GPH BY GROUP AND BY PERIOD

	TEST GROUP GPH	CONTROL GROUP GPH	
FY 2015 P1	1.00	0.96	
FY 2015 P2	0.95	0.92	
FY 2015 P3	0.93	0.92	
FY 2015 P4	0.96	0.89	
FY 2015 P5	0.85	0.85	
FY 2015 P6	0.80	0.81	
FY 2015 P7	0.81	0.77	
FY 2015 P8	0.76	0.76	
FY 2015 P9	0.85	0.79	
FY 2015 P10	0.89	0.93	
FY 2015 P11	0.89	0.86	
FY 2015 P12			
FY 2016 P1	0.96	0.99	TECHNOLOGY INSTALLED ON TEST GROUP TRAILERS DURING FY 2016 P2
FY 2016 P2	0.93	0.97	
FY 2016 P3	0.93	1.02	
FY 2016 P4	0.86	0.94	
FY 2016 P5	0.79	0.85	
FY 2016 P6	0.70	0.78	
FY 2016 P7	0.63	0.72	
FY 2016 P8	0.65	0.74	
FY 2016 P9	0.76	0.81	
FY 2016 P10	0.73	0.82	
FY 2016 P11	0.79	0.86	
FY 2016 P12	0.84	0.93	
FY 2017 P1	0.89	0.99	
FY 2017 P2	0.87	0.96	

Sygma Network Refrigerated Trailers / Oklahoma City Terminal
Gallons and Hours by Trailer and Period
WorldKlass Infrared Fuel Excitation System installed on Test Group trailers During FY 2016 P1
Version 1.0 2018-05-02

	FY 2015 P1			FY 2015 P2			FY 2015 P3			FY 2015 P4		
TRAILER NUMBER	GALLONS	HOURS	GPH CALC	GALLONS	HOURS	GPH CALC	GALLONS	HOURS	GPH CALC	GALLONS	HOURS	GPH CALC
TEST GROUP (WITH TECHNOLOGY CANISTERS)												
242257	281.1	326	0.86	191.8	211	0.91	305.4	396	0.77	253.1	220	1.15
216660	309.1	351	0.88	281.0	315	0.89	414.0	442	0.94	198.4	273	0.73
216661	370.0	331	1.12	272.4	275	0.99	401.4	460	0.87	378.5	278	1.36
216669	313.8	324	0.97	374.0	454	0.82	371.0	426	0.87	253.7	306	0.83
216674	224.0	261	0.86	344.0	450	0.76	310.4	251	1.24	286.0	337	0.85
216675	312.0	307	1.02	309.8	350	0.89	360.3	405	0.89	250.4	321	0.78
216676	297.7	319	0.93	300.9	352	0.85	346.0	452	0.77	407.3	376	1.08
216677	405.6	384	1.06	356.0	302	1.18	405.2	340	1.19	245.1	210	1.17
216679	233.2	245	0.95	395.2	390	1.01	302.5	372	0.81	260.0	300	0.87
216681	324.4	327	0.99	342.2	344	0.99	344.1	353	0.97	117.0	128	0.91
217022	215.9	247	0.87	447.0	421	1.06	417.0	430	0.97	200.4	202	0.99
217023	344.2	412	0.84	228.2	281	0.81	427.0	484	0.88	237.4	263	0.90
217024	405.0	370	1.09	407.8	412	0.99	436.9	371	1.18	292.0	264	1.11
217025	226.9	217	1.05	183.2	211	0.87	422.3	444	0.95	294.0	342	0.86
217026	244.1	249	0.98	353.5	333	1.06	388.2	439	0.88	167.0	172	0.97
217374	387.0	346	1.12	310.2	346	0.90	415.4	408	1.02	234.1	260	0.90
219486	330.9	258	1.28	291.5	272	1.07	468.0	502	0.93	288.1	302	0.95
219488	163.0	164	0.99	335.6	333	1.01	335.1	355	0.94	198.6	219	0.91
219502	231.3	228	1.01	353.0	343	1.03	236.1	274	0.86	152.0	156	0.97
219516	304.0	317	0.96	303.0	266	1.14	239.0	258	0.93	215.7	243	0.89
239847	299.0	215	1.39	263.0	301	0.87	303.0	323	0.94	170.0	137	1.24
TEST GROUP TOTALS	6222.2	6198	1.00	6643.3	6962	0.95	7648.3	8185	0.93	5098.8	5309	0.96
CONTROL GROUP (WITHOUT TECHNOLOGY CANISTERS)												
242256	214.2	195	1.10	278.4	201	1.39	297.1	328	0.91	213.0	219	0.97
216652	392.0	367	1.07	320.5	391	0.82	395.0	474	0.83	230.3	164	1.40
216654	349.2	353	0.99	379.0	327	1.16	463.0	415	1.12	266.0	248	1.07
216655	311.0	347	0.90	296.2	295	1.00	322.0	355	0.91	197.0	265	0.74
216656	374.0	421	0.89	315.4	326	0.97	402.0	508	0.79	262.0	385	0.68
216657	263.0	276	0.95	387.4	240	1.61	334.0	314	1.06	347.0	304	1.14
216658	381.7	398	0.96	303.2	261	1.16	437.8	414	1.06	218.0	268	0.81
216659	227.0	238	0.95	307.0	367	0.84	323.8	391	0.83	197.0	253	0.78
216662	371.8	407	0.91	274.7	322	0.85	376.9	386	0.98	261.5	263	0.99
216663	250.5	273	0.92							276.0	67	4.12
216664	332.9	349	0.95	299.8	295	1.02	498.9	506	0.99	181.0	154	1.18
216665	237.5	315	0.75	306.5	331	0.93	269.5	368	0.73	267.0	288	0.93
216666	332.5	254	1.31	248.3	327	0.76	431.0	448	0.96	162.1	268	0.60
216667	298.0	295	1.01	436.0	389	1.12	420.8	398	1.06	357.6	328	1.09
216668	344.0	295	1.17	354.4	352	1.01	205.0	195	1.05	265.2	318	0.83
216670	338.0	228	1.48	258.0	270	0.96	334.0	350	0.95	294.7	297	0.99
216671	269.3	341	0.79	258.0	278	0.93	393.4	439	0.90	254.0	264	0.96
216672	313.0	337	0.93	294.0	1040	0.28				366.6	1062	0.35
216673	341.2	385	0.89	237.0	255	0.93	438.2	532	0.82	228.4	228	1.00
216678	325.5	423	0.77	370.2	394	0.94	405.2	412	0.98	204.3	213	0.96
216680	316.7	333	0.95	412.2	435	0.95	296.0	337	0.88	283.0	303	0.93
216682	375.1	416	0.90	340.1	252	1.35	323.8	479	0.68	233.2	241	0.97
217335	186.7	206	0.91	251.0	265	0.95	476.0	467	1.02	396.4	327	1.21
217372	400.4	359	1.12	295.0	309	0.95	398.1	432	0.92	369.0	376	0.98
217378	376.0	407	0.92	274.2	269	1.02	374.8	409	0.92	317.1	327	0.97
228730	248.3	296	0.84	292.1	313	0.93	277.1	319	0.87	203.0	243	0.84
219489	293.0	355	0.83	383.5	412	0.93	297.0	290	1.02	290.6	376	0.77
219507	236.0	222	1.06	334.3	338	0.99	378.0	409	0.92	179.0	173	1.03
219515	205.6	215	0.96	339.0	383	0.89	346.0	391	0.88	227.0	240	0.95
219532	202.2	203	1.00	293.7	292	1.01	292.1	291	1.00	164.0	176	0.93
CONTROL GROUP TOTALS	9106.3	9509	0.96	9139.1	9929	0.92	10206.5	11057	0.92	7711.0	8638	0.89

FY 2015 P5			FY 2015 P6			FY 2015 P7			FY 2015 P8		
GALLONS	HOURS	GPH CALC	GALLONS	HOURS	GPH CALC	GALLONS	HOURS	GPH CALC	GALLONS	HOURS	GPH CALC
103.1	156	0.66	146.0	184	0.79	81.2	96	0.85	74.0	94	0.79
181.8	204	0.89	197.8	236	0.84	119.0	174	0.68	121.0	158	0.77
159.0	182	0.87	176.0	213	0.83	91.7	129	0.71	127.7	197	0.65
209.0	352	0.59	200.0	171	1.17	161.8	186	0.87	148.0	201	0.74
180.6	221	0.82	229.9	319	0.72	165.6	228	0.73	102.0	106	0.96
151.0	186	0.81	140.6	277	0.51	137.2	185	0.74	106.2	164	0.65
183.1	243	0.75	182.0	241	0.76	123.1	169	0.73	178.0	209	0.85
151.1	172	0.88	189.5	182	1.04	157.8	218	0.72	139.2	147	0.95
243.5	175	1.39	202.1	249	0.81	99.0	142	0.70	138.7	172	0.81
118.2	151	0.78	210.3	238	0.88	333.0	231	1.44	110.8	184	0.60
162.4	186	0.87	166.0	208	0.80	170.1	189	0.90	161.6	180	0.90
117.5	131	0.90	161.1	265	0.61	129.1	172	0.75	111.1	154	0.72
199.0	234	0.85	147.7	277	0.53	105.0	146	0.72	86.2	123	0.70
137.0	173	0.79	163.0	163	1.00	66.1	90	0.73	105.0	142	0.74
152.3	237	0.64	113.5	130	0.87	60.0	79	0.76	37.0	38	0.97
143.0	196	0.73	241.2	234	1.03	123.0	160	0.77	115.1	146	0.79
225.8	180	1.25	129.0	171	0.75	57.1	57	1.00	102.8	135	0.76
183.7	221	0.83	144.2	159	0.91	103.0	139	0.74	120.6	214	0.56
168.1	154	1.09	195.2	276	0.71	79.0	122	0.65	137.0	180	0.76
224.0	261	0.86	231.3	251	0.92	57.0	83	0.69			
125.0	143	0.87	116.7	135	0.86	46.4	60	0.77	52.1	66	0.79
3518.2	4158	0.85	3683.1	4579	0.80	2465.2	3055	0.81	2274.1	3010	0.76
178.1	204	0.87	138.9	149	0.93	76.0	121	0.63	86.0	79	1.09
232.0	264	0.88	219.6	235	0.93	89.6	87	1.03	96.0	105	0.91
151.5	188	0.81	182.0	173	1.05	126.5	140	0.90	137.4	138	1.00
150.0	191	0.79	284.4	384	0.74	161.6	223	0.72	116.0	196	0.59
113.4	93	1.22	184.2	262	0.70	106.2	146	0.73	167.6	190	0.88
228.1	272	0.84	289.5	291	0.99	157.0	196	0.80	142.1	199	0.71
148.0	104	1.42	164.0	149	1.10	130.0	162	0.80	135.4	185	0.73
145.2	166	0.87	193.8	281	0.69	85.0	96	0.89	196.1	271	0.72
213.8	206	1.04	313.0	234	1.34	130.2	205	0.64	69.9	121	0.58
176.2	188	0.94	230.1	295	0.78	164.3	246	0.67	123.0	167	0.74
164.2	236	0.70	203.0	293	0.69	106.0	107	0.99	114.0	145	0.79
142.3	213	0.67	123.0	145	0.85	85.1	84	1.01	80.0	81	0.99
109.0	185	0.59	178.0	229	0.78	92.7	174	0.53	77.5	123	0.63
241.7	245	0.99	306.1	321	0.95	160.1	194	0.83	212.9	202	1.05
227.9	256	0.89	240.3	373	0.64	162.1	252	0.64	191.6	239	0.80
138.9	155	0.90	178.6	260	0.69	145.4	179	0.81	119.2	166	0.72
174.3	290	0.60	134.1	231	0.58	158.0	181	0.87	113.3	121	0.94
153.0	208	0.74	192.9	327	0.59	164.4	207	0.79	61.3	93	0.66
180.8	177	1.02	269.4	273	0.99	125.9	164	0.77	154.8	187	0.83
138.8	162	0.86	272.2	235	1.16	185.4	214	0.87	75.0	119	0.63
186.4	253	0.74	197.1	274	0.72	67.0	96	0.70	84.7	112	0.76
177.0	193	0.92	105.0	133	0.79	123.2	161	0.77	112.0	131	0.85
168.2	191	0.88	94.9	118	0.80	97.0	128	0.76	74.1	93	0.80
192.2	241	0.80	221.0	293	0.75	122.2	180	0.68	129.9	156	0.83
180.0	223	0.81	138.2	190	0.73	127.1	204	0.62	113.0	142	0.80
208.9	247	0.85	181.0	279	0.65	117.6	158	0.74	79.0	130	0.61
125.0	125	1.00	190.0	292	0.65	58.0	99	0.59	129.0	159	0.81
190.5	228	0.84	129.0	128	1.01	41.0	65	0.63	96.1	117	0.82
150.1	177	0.85	129.0	162	0.80	105.3	58	1.82	120.2	304	0.40
4985.5	5881	0.85	5682.3	7009	0.81	3469.9	4527	0.77	3407.1	4471	0.76

FY 2015 P9			FY 2015 P10			FY 2015 P11			FY 2016 P1		
GALLONS	HOURS	GPH CALC	GALLONS	HOURS	GPH CALC	GALLONS	HOURS	GPH CALC	GALLONS	HOURS	GPH CALC
220.4	240	0.92	191.4	257	0.74	189.5	209	0.91	359.0	356	1.01
93.0	127	0.73	207.0	256	0.81	222.0	325	0.68	292.8	373	0.78
290.0	330	0.88	190.0	251	0.76	201.3	255	0.79			
234.9	278	0.84	315.4	340	0.93	252.7	290	0.87	284.8	278	1.02
175.8	180	0.98	154.0	233	0.66	231.9	238	0.97	249.4	267	0.93
176.0	206	0.85	259.5	258	1.01	191.8	250	0.77	335.0	382	0.88
252.4	227	1.11	278.2	329	0.85	274.0	267	1.03	296.1	342	0.87
149.7	135	1.11	302.3	323	0.94	257.1	278	0.92	375.9	327	1.15
141.0	170	0.83	191.8	208	0.92	291.6	267	1.09	183.1	183	1.00
108.0	193	0.56	168.6	169	1.00	182.2	190	0.96	346.1	333	1.04
199.9	249	0.80	147.0	134	1.10	192.1	166	1.16			
233.0	316	0.74	245.6	84	2.92	122.5	345	0.36			
193.2	230	0.84	211.0	269	0.78	252.8	253	1.00	332.4	310	1.07
119.1	157	0.76	130.1	139	0.94	201.0	174	1.16	365.5	400	0.91
105.0	131	0.80	155.2	182	0.85	105.0	150	0.70	286.5	299	0.96
188.0	225	0.84	227.0	201	1.13	272.0	270	1.01	294.8	303	0.97
258.9	240	1.08	126.0	141	0.89	224.0	256	0.88	381.9	371	1.03
			187.2	348	0.54	241.8	264	0.92	291.7	341	0.86
185.0	268	0.69	217.5	268	0.81	157.0	187	0.84	387.6	419	0.93
59.0	77	0.77	145.2	151	0.96	141.0	128	1.10	402.9	397	1.01
131.1	173	0.76	150.0	178	0.84	196.0	189	1.04	413.6	431	0.96
3513.4	4152	0.85	4200.0	4719	0.89	4399.3	4951	0.89	5879.1	6112.0	0.96
137.1	202	0.68	193.5	187	1.03	115.0	128	0.90	282.8	268	1.06
160.0	172	0.93	205.0	240	0.85	341.0	334	1.02			
161.9	167	0.97	136.5	125	1.09	239.1	239	1.00			
145.9	194	0.75	254.3	267	0.95	327.0	413	0.79			
110.0	146	0.75	160.6	206	0.78	206.0	255	0.81			
301.0	307	0.98	145.2	190	0.76	232.1	311	0.75			
152.0	170	0.89	201.0	243	0.83	239.5	279	0.86			
203.6	219	0.93	311.1	232	1.34	321.9	366	0.88			
126.9	173	0.73	298.5	338	0.88	267.2	289	0.92			
201.0	231	0.87	112.3	57	1.97	297.9	526	0.57			
176.3	266	0.66	214.1	290	0.74	240.1	304	0.79			
162.0	196	0.83	203.0	282	0.72	227.2	168	1.35	289.4	318	0.91
127.9	216	0.59	152.0	207	0.73	179.0	236	0.76	274.7	294	0.93
157.1	236	0.67	151.0	193	0.78	161.0	173	0.93	365.2	353	1.03
243.3	363	0.67	336.8	326	1.03	310.1	389	0.80	379.8	350	1.09
286.0	329	0.87	390.0	303	1.29	412.5	421	0.98	390.2	356	1.10
219.0	275	0.80	146.0	146	1.00	294.6	210	1.40	266.8	283	0.94
			157.0	248	0.63	180.0	264	0.68	181.4	212	0.86
						51.1	127	0.40	185.5	160	1.16
153.6	178	0.86	212.0	214	0.99	286.2	319	0.90	302.1	287	1.05
124.9	178	0.70	239.0	255	0.94	288.5	245	1.18	408.1	346	1.18
187.0	258	0.72	242.0	288	0.84	223.0	245	0.91	277.8	324	0.86
200.0	212	0.94	280.4	294	0.95	191.3	272	0.70			
246.1	294	0.84	253.4	275	0.92	258.6	266	0.97	353.9	355	1.00
196.6	256	0.77	247.7	322	0.77	217.0	303	0.72	442.5	467	0.95
165.1	226	0.73	130.6	167	0.78	153.0	144	1.06	345.3	376	0.92
130.2	176	0.74	189.3	238	0.80	251.0	354	0.71	389.8	434	0.90
207.4	274	0.76	161.1	184	0.88	211.0	244	0.86	329.8	326	1.01
179.0	230	0.78	142.1	157	0.91	153.0	172	0.89	246.4	257	0.96
130.6	158	0.83	423.3	274	1.54	202.3	239	0.85	251.4	250	1.01
4991.5	6302	0.79	6288.8	6748	0.93	7077.2	8235	0.86	5962.9	6016.0	0.99

FY 2016 P2			FY 2016 P3			FY 2016 P4			FY 2016 P5		
GALLONS	HOURS	GPH CALC	GALLONS	HOURS	GPH CALC	GALLONS	HOURS	GPH CALC	GALLONS	HOURS	GPH CALC
327.1	371	0.88	260.1	258	1.01	196.3	220	0.89	98.2	129	0.76
245.8	258	0.95							67.0	78	0.86
259.3	272	0.95	135.0	145	0.93	177.1	212	0.84	166.5	214	0.78
280.9	288	0.98	310.6	328	0.95	243.5	291	0.84	123.7	135	0.92
348.8	349	1.00	266.5	277	0.96	202.4	248	0.82	145.1	184	0.79
131.1	176	0.74				258.6	325	0.80	178.3	209	0.85
424.7	441	0.96	326.5	346	0.94	203.3	231	0.88	239.2	290	0.82
171.0	185	0.92	95.6	93	1.03	263.9	312	0.85	189.0	227	0.83
34.7	32	1.08	126.7	125	1.01	198.7	232	0.86	125.0	142	0.88
387.4	433	0.89	279.9	296	0.95	211.8	251	0.84	196.2	231	0.85
206.5	218	0.95	265.6	289	0.92	292.9	352	0.83	233.8	397	0.59
282.8	313	0.90	283.2	315	0.90	182.8	194	0.94	169.3	219	0.77
335.3	337	0.99	289.7	317	0.91	182.7	200	0.91	138.1	185	0.75
403.9	463	0.87	155.8	217	0.72	259.5	299	0.87	232.0	313	0.74
402.2	401	1.00	382.4	402	0.95	164.2	180	0.91			
204.9	223	0.92	162.9	170	0.96	223.0	227	0.98	164.8	188	0.88
262.2	287	0.91	167.3	188	0.89	158.0	215	0.73	100.0	129	0.78
333.4	378	0.88	318.6	341	0.93	211.2	234	0.90	161.0	215	0.75
251.6	242	1.04	244.0	253	0.96	135.7	193	0.70	128.2	157	0.82
289.1	344	0.84	349.5	388	0.90	233.8	252	0.93	111.1	128	0.87
5582.7	6011	0.93	4419.9	4748	0.93	3999.4	4668	0.86	2966.5	3770	0.79
261.7	255	1.03	348.4	314	1.11	185.1	229	0.81	166.1	210	0.79
256.0	253	1.01	214.5	217	0.99	150.5	159	0.95	181.9	260	0.70
244.1	272	0.90	189.2	170	1.11	237.0	193	1.23	136.9	161	0.85
290.2	347	0.84	260.3	284	0.92				106.0	109	0.97
386.9	405	0.96	258.3	261	0.99	150.4	159	0.95	169.1	222	0.76
353.0	364	0.97	201.8	195	1.03	48.0	54	0.89	76.2	107	0.71
418.6	448	0.93	219.5	193	1.14	174.0	165	1.05	160.9	171	0.94
194.6	205	0.95	176.3	184	0.96	250.8	265	0.95	175.8	225	0.78
223.3	227	0.98	185.4	192	0.97	250.2	267	0.94	197.1	233	0.85
308.4	324	0.95	206.4	201	1.03	133.5	154	0.87	129.3	161	0.80
257.7	256	1.01	293.5	305	0.96	198.6	216	0.92	189.2	204	0.93
338.6	389	0.87	172.5	175	0.99	230.5	267	0.86	184.9	216	0.86
285.6	308	0.93	191.5	174	1.10	92.7	104	0.89	148.1	163	0.91
321.1	322	1.00	279.6	264	1.06	269.1	294	0.92	234.1	302	0.78
307.0	326	0.94	258.1	239	1.08	242.4	221	1.10	168.6	174	0.97
298.5	329	0.91	251.8	242	1.04	158.8	175	0.91	121.7	136	0.89
286.1	302	0.95	244.6	246	0.99	312.2	338	0.92	180.0	194	0.93
			210.5	198	1.06	92.2	92	1.00			
300.8	308	0.98	306.5	317	0.97	166.7	184	0.91	96.2	123	0.78
420.2	395	1.06	418.5	395	1.06	378.0	340	1.11	224.8	241	0.93
362.6	352	1.03	397.8	381	1.04	295.9	315	0.94	130.2	156	0.83
266.8	282	0.95	270.8	249	1.09	105.1	108	0.97	224.9	263	0.86
339.8	338	1.01	225.4	239	0.94	245.4	287	0.86	185.7	203	0.91
392.5	403	0.97	280.9	279	1.01	268.1	286	0.94	305.8	350	0.87
209.9	194	1.08	291.5	220	1.33	274.0	286	0.96	205.1	249	0.82
337.0	335	1.01	336.1	350	0.96	216.1	243	0.89	149.4	196	0.76
296.5	304	0.98	344.3	335	1.03	177.0	195	0.91	154.0	190	0.81
307.7	293	1.05	250.4	261	0.96	268.9	302	0.89	152.3	175	0.87
314.3	303	1.04	186.1	203	0.92	249.5	263	0.95	95.1	114	0.83
334.7	317	1.06	262.1	268	0.98	158.3	173	0.92	122.0	138	0.88
8914.2	9156	0.97	7732.6	7551	1.02	5979.0	6334	0.94	4771.4	5646	0.85

FY 2016 P6			FY 2016 P7			FY 2016 P8			FY 2016 P9		
GALLONS	HOURS	GPH CALC	GALLONS	HOURS	GPH CALC	GALLONS	HOURS	GPH CALC	GALLONS	HOURS	GPH CALC
95.7	139	0.69	69.0	97	0.71	170.2	217	0.78	247.9	345	0.72
156.7	279	0.56	90.4	163	0.55	77.8	124	0.63	206.9	311	0.67
102.0	148	0.69	83.1	132	0.63	90.1	116	0.78	209.5	270	0.78
145.7	241	0.60	153.3	216	0.71	106.6	158	0.67	284.1	329	0.86
119.2	176	0.68	80.1	114	0.70	137.6	193	0.71	249.7	314	0.80
190.6	258	0.74	141.2	224	0.63	159.5	268	0.60	298.7	338	0.88
192.2	282	0.68	142.7	225	0.63	177.9	272	0.65	235.6	293	0.80
188.9	272	0.69	128.6	169	0.76	178.2	224	0.80	260.2	347	0.75
180.1	224	0.80	118.1	162	0.73	55.6	77	0.72	238.5	322	0.74
102.0	149	0.68	130.1	205	0.63	100.2	138	0.73	214.1	276	0.78
261.5	307	0.85									
87.0	172	0.51	181.2	314	0.58	130.1	241	0.54	289.0	446	0.65
181.3	221	0.82	138.3	184	0.75	126.5	193	0.66	38.3	46	0.83
205.5	274	0.75	367.3	633	0.58	258.6	432	0.60	216.3	285	0.76
167.5	262	0.64	210.8	406	0.52	118.5	230	0.52	274.4	370	0.74
114.8	193	0.59	133.1	207	0.64	189.3	251	0.75	244.8	298	0.82
119.3	146	0.82	68.3	94	0.73	133.9	180	0.74	132.8	148	0.90
150.2	211	0.71	136.2	189	0.72	89.2	124	0.72	235.1	290	0.81
195.4	279	0.70	85.1	139	0.61	163.7	332	0.49	191.7	296	0.65
104.6	143	0.73	68.0	129	0.53	89.7	145	0.62	182.2	231	0.79
			58.2	81	0.72	40.0	49	0.82	82.9	162	0.51
3060.2	4376	0.70	2583.1	4083	0.63	2593.2	3964	0.65	4332.7	5717	0.76
146.7	177	0.83	145.8	215	0.68	164.0	208	0.79	285.8	348	0.82
179.1	224	0.80	66.9	94	0.71	150.7	188	0.80	204.8	248	0.83
151.4	131	1.16	64.9	74	0.88	132.1	151	0.87	210.9	232	0.91
161.7	249	0.65	62.5	92	0.68	109.1	157	0.69	193.6	252	0.77
69.0	92	0.75	65.1	93	0.70	87.1	133	0.65	181.5	281	0.65
			75.5	131	0.58	61.7	89	0.69	305.9	350	0.87
122.1	165	0.74	89.0	113	0.79	95.0	120	0.79	235.2	276	0.85
168.9	235	0.72	107.7	146	0.74	157.6	210	0.75	224.6	283	0.79
184.0	221	0.83	153.1	177	0.86	158.4	208	0.76	275.8	331	0.83
156.6	201	0.78	96.4	119	0.81	129.3	189	0.68	273.7	297	0.92
177.5	218	0.81	68.1	128	0.53	136.1	189	0.72	242.7	324	0.75
41.0	47	0.87	56.3	69	0.82	126.1	158	0.80	321.0	358	0.90
95.7	142	0.67	106.1	128	0.83	106.2	131	0.81	159.0	179	0.89
208.3	315	0.66	213.8	305	0.70	271.1	380	0.71	316.2	416	0.76
273.0	363	0.75	240.6	309	0.78	209.0	285	0.73	80.3	84	0.96
147.6	215	0.69	87.0	120	0.73	119.8	174	0.69	84.6	92	0.92
171.4	274	0.63	68.3	90	0.76	100.7	136	0.74	193.9	241	0.80
85.1	130	0.65	99.6	164	0.61	109.7	150	0.73	136.0	174	0.78
140.7	197	0.71	84.2	95	0.89	102.5	141	0.73	119.9	150	0.80
124.3	167	0.74	154.0	204	0.75	222.6	257	0.87	317.4	356	0.89
259.2	261	0.99	133.8	190	0.70	206.9	234	0.88	293.2	304	0.96
178.4	205	0.87	179.8	238	0.76	146.9	196	0.75	326.2	399	0.82
225.2	225	1.00	119.3	155	0.77	87.0	141	0.62	200.8	217	0.93
190.3	223	0.85	77.9	100	0.78	103.0	121	0.85	294.0	346	0.85
226.5	298	0.76	82.1	133	0.62	122.9	146	0.84	282.1	383	0.74
73.9	119	0.62	118.7	178	0.67	128.5	187	0.69	226.2	343	0.66
128.0	176	0.73	138.3	231	0.60	171.0	257	0.67	164.1	251	0.65
113.2	148	0.76	136.8	216	0.63	125.0	159	0.79	204.4	245	0.83
120.4	155	0.78	108.9	130	0.84	98.7	161	0.61	180.7	229	0.79
144.3	178	0.81	121.0	187	0.65	313.3	470	0.67	374.3	531	0.70
4463.5	5751	0.78	3321.5	4624	0.72	4252.0	5726	0.74	6908.8	8520	0.81

FY 2016 P10			FY 2016 P11			FY 2016 P12			FY 2017 P1		
GALLONS	HOURS	GPH CALC	GALLONS	HOURS	GPH CALC	GALLONS	HOURS	GPH CALC	GALLONS	HOURS	GPH CALC
218.4	295	0.74	205.4	228	0.90	493.3	558	0.88	376	411	0.91
215.1	308	0.70	212.1	254	0.84	500.3	485	1.03	396	483	0.82
307.0	459	0.67	225.9	291	0.78	395.3	499	0.79	167	196	0.85
207.4	289	0.72	84.3	98	0.86	522.0	633	0.82	237	276	0.86
192.0	257	0.75	158.6	241	0.66	569.7	637	0.89	417	437	0.95
230.3	262	0.88	269.3	345	0.78	316.4	357	0.89	341	392	0.87
218.5	328	0.67	214.3	254	0.84	505.5	576	0.88	311	316	0.98
123.8	187	0.66	114.3	192	0.60	261.2	346	0.75			
116.9	140	0.84	193.8	232	0.84	455.1	553	0.82	423	465	0.91
171.4	285	0.60	190.5	247	0.77	502.5	596	0.84	258	288	0.90
			181.8	243	0.75						
130.5	169	0.77	230.5	307	0.75	415.1	492	0.84	386	437	0.88
185.9	227	0.82	149.9	216	0.69	300.7	428	0.70	245	232	1.06
198.9	272	0.73	251.5	308	0.82	539.9	615	0.88	303	351	0.86
246.2	331	0.74	261.9	329	0.80	444.8	589	0.76	319	360	0.89
228.0	292	0.78	286.8	358	0.80	521.1	623	0.84	385	447	0.86
			172.7	185	0.93	295.1	369	0.80	262	271	0.97
142.4	200	0.71	208.5	256	0.81	417.9	492	0.85	325	434	0.75
104.5	177	0.59	263.5	309	0.85	401.0	486	0.83	323	395	0.82
258.8	312	0.83	131.0	167	0.78	520.3	636	0.82	384	380	1.01
198.9	246	0.81	199.4	258	0.77				281	321	0.88
3694.9	5036	0.73	4206.0	5318	0.79	8377.2	9970	0.84	6139	6892	0.89
210.4	230	0.91	233.1	259	0.90	289.0	347	0.83	331	318	1.04
187.0	201	0.93	31.9	43	0.74						
158.0	217	0.73	241.7	269	0.90	520.9	489	1.07	323	329	0.98
196.1	253	0.78	190.4	271	0.70	472.8	543	0.87	293	320	0.92
211.1	272	0.78	174.3	219	0.80	575.6	528	1.09	334	371	0.90
182.0	237	0.77	210.2	226	0.93	439.7	508	0.87	403	363	1.11
272.9	304	0.90	284.2	313	0.91	516.7	537	0.96	268	271	0.99
181.3	254	0.71	202.3	251	0.81	208.5	245	0.85	254	280	0.91
191.9	257	0.75	276.4	266	1.04	567.8	568	1.00	556	440	1.26
184.2	259	0.71	148.9	166	0.90	402.8	455	0.89	343	358	0.96
224.8	306	0.73	225.1	263	0.86	520.8	601	0.87	309	282	1.10
192.3	194	0.99	283.4	345	0.82	604.2	570	1.06	418	433	0.97
143.3	176	0.81	81.1	89	0.91	447.5	492	0.91	451	377	1.20
183.3	224	0.82	362.2	419	0.86	156.8	150	1.05			
			67.5	51	1.32						
			73.6	88	0.84	433.6	524	0.83	308	327	0.94
206.4	254	0.81	250.0	304	0.82	496.0	509	0.97	451	469	0.96
204.8	257	0.80	188.9	218	0.87	512.6	606	0.85	281	276	1.02
213.8	275	0.78	236.6	291	0.81	705.8	707	1.00	361	391	0.92
141.2	144	0.98	315.5	374	0.84	386.7	345	1.12	379	396	0.96
196.5	264	0.74	213.5	240	0.89	467.2	534	0.87	274	270	1.01
143.6	197	0.73	194.1	216	0.90	573.0	632	0.91	225	227	0.99
110.1	108	1.02	238.1	261	0.91	447.9	436	1.03	321	320	1.00
372.4	349	1.07	283.4	321	0.88	524.1	669	0.78	358	414	0.86
124.2	171	0.73	203.5	276	0.74	451.7	537	0.84	305	334	0.91
244.0	293	0.83	232.5	268	0.87	492.2	567	0.87	372	358	1.04
153.4	195	0.79	193.4	238	0.81	425.6	525	0.81	202	304	0.66
230.9	263	0.88	215.1	230	0.94	541.3	626	0.86	270	281	0.96
192.0	227	0.85	207.7	246	0.84	508.6	526	0.97	356	375	0.95
138.3	160	0.86	200.4	220	0.91	479.4	451	1.06	344	286	1.20
5390.2	6541	0.82	6259.0	7241	0.86	13168.8	14227	0.93	9090	9170	0.99

FY 2017 P2		
GALLONS	HOURS	GPH CALC
230.0	283	0.81
275.8	328	0.84
405.2	442	0.92
418.9	498	0.84
414.8	473	0.88
35.0	35	1.00
67.5	76	0.89
285.8	271	1.05
304.5	375	0.81
339.6	377	0.90
275.0	383	0.72
266.2	299	0.89
356.7	412	0.87
371.8	445	0.84
320.5	368	0.87
384.4	426	0.90
143.8	145	0.99
336.9	393	0.86
260.0	314	0.83
5492.4	6343	0.87
348.1	274	1.27
254.5	278	0.92
274.5	296	0.93
333.8	409	0.82
407.5	294	1.39
361.8	352	1.03
350.5	376	0.93
524.6	436	1.20
310.1	343	0.90
430.7	496	0.87
373.6	372	1.00
362.6	374	0.97
53.0	40	1.33
390.5	460	0.85
338.7	426	0.80
331.6	385	0.86
332.9	365	0.91
328.0	325	1.01
357.6	389	0.92
412.9	451	0.92
364.0	378	0.96
355.9	372	0.96
340.7	393	0.87
289.8	365	0.79
438.4	461	0.95
265.4	317	0.84
272.1	256	1.06
381.3	329	1.16
9585.1	10012	0.96

ATTACHMENT F

T-Test Results Table

Independent Samples Test

		Levene's Test for Equality of Variances		t-test for Equality of Means						
									95% Confidence Interval of the Difference	
		F	Sig.	t	df	Sig. (2-tailed)	Mean Difference	Std. Error Difference	Lower	Upper
GPH 2015 P1	Equal variances assumed	.042	.839	-.908	49	.368	-.03781	.04164	-.12149	.04588
	Equal variances not assumed			-.925	45.778	.360	-.03781	.04090	-.12014	.04452
GPH 2015 P2	Equal variances assumed	1.080	.304	.576	48	.567	.03079	.05341	-.07659	.13817
	Equal variances not assumed			.636	43.377	.528	.03079	.04840	-.06680	.12838
GPH 2015 P3	Equal variances assumed	.041	.840	-.378	47	.707	-.01250	.03310	-.07909	.05409
	Equal variances not assumed			-.368	38.510	.715	-.01250	.03398	-.08127	.05627
GPH 2015 P4	Equal variances assumed	1.298	.260	.485	49	.630	.06662	.13742	-.20953	.34277
	Equal variances not assumed			.568	34.341	.574	.06662	.11729	-.17166	.30490
GPH 2015 P5	Equal variances assumed	.033	.856	.210	48	.835	.01059	.05043	-.09081	.11200
	Equal variances not assumed			.206	40.458	.837	.01059	.05129	-.09304	.11422
GPH 2015 P6	Equal variances assumed	.936	.338	.085	48	.932	.00429	.05031	-.09687	.10544
	Equal variances not assumed			.087	46.037	.931	.00429	.04930	-.09495	.10352
GPH 2015 P7	Equal variances assumed	.524	.473	.137	48	.892	.00818	.05985	-.11216	.12851
	Equal variances not assumed			.144	47.995	.886	.00818	.05691	-.10624	.12259
GPH 2015 P8	Equal variances assumed	1.448	.235	.217	47	.829	.00872	.04019	-.07213	.08958
	Equal variances not assumed			.229	46.669	.820	.00872	.03809	-.06791	.08536
GPH 2015 P9	Equal variances assumed	.501	.483	-1.429	46	.160	-.05021	.03515	-.12096	.02053
	Equal variances not assumed			-1.358	33.058	.184	-.05021	.03698	-.12544	.02501
GPH 2015 P10	Equal variances assumed	.159	.692	-.138	48	.891	-.01461	.10574	-.22722	.19799
	Equal variances not assumed			-.128	30.152	.899	-.01461	.11434	-.24809	.21886
GPH 2015 P11	Equal variances assumed	.032	.858	-.618	49	.540	-.03438	.05566	-.14624	.07748
	Equal variances not assumed			-.627	45.398	.534	-.03438	.05482	-.14477	.07601
GPH 2016 P1	Equal variances assumed	.263	.611	1.027	35	.311	.03079	.02997	-.03005	.09162
	Equal variances not assumed			1.029	34.995	.310	.03079	.02991	-.02993	.09151
GPH 2016 P2	Equal variances assumed	.328	.570	2.867	46	.006	.05285	.01843	.01575	.08995
	Equal variances not assumed			2.764	33.856	.009	.05285	.01912	.01399	.09171
GPH 2016 P3	Equal variances assumed	.015	.903	3.897	48	.000	.09000	.02310	.04356	.13644
	Equal variances not assumed			3.953	42.831	.000	.09000	.02277	.04408	.13592
GPH 2016 P4	Equal variances assumed	.139	.711	3.694	46	.001	.08623	.02334	.03924	.13321
	Equal variances not assumed			3.873	44.088	.000	.08623	.02227	.04135	.13110
GPH 2016 P5	Equal variances assumed	.008	.930	2.707	46	.009	.05579	.02061	.01431	.09727
	Equal variances not assumed			2.657	36.203	.012	.05579	.02100	.01322	.09836
GPH 2016 P6	Equal variances assumed	.802	.375	2.700	47	.010	.08500	.03149	.02166	.14834
	Equal variances not assumed			2.843	46.571	.007	.08500	.02990	.02484	.14516

GPH 2016 P7	Equal variances assumed	.713	.403	3.040	48	.004	.07600	.02500	.02574	.12626
	Equal variances not assumed			3.170	46.015	.003	.07600	.02397	.02775	.12425
GPH 2016 P8	Equal variances assumed	1.903	.174	2.891	48	.006	.06917	.02392	.02107	.11726
	Equal variances not assumed			2.752	33.956	.009	.06917	.02513	.01810	.12024
GPH 2016 P9	Equal variances assumed	.014	.907	2.294	48	.026	.05867	.02557	.00725	.11009
	Equal variances not assumed			2.274	39.607	.028	.05867	.02580	.00650	.11084
GPH 2016 P10	Equal variances assumed	1.335	.254	3.348	45	.002	.09102	.02719	.03626	.14577
	Equal variances not assumed			3.502	43.839	.001	.09102	.02599	.03863	.14340
GPH 2016 P11	Equal variances assumed	.242	.625	3.102	49	.003	.08471	.02731	.02984	.13959
	Equal variances not assumed			3.295	48.987	.002	.08471	.02571	.03304	.13638
GPH 2016 P12	Equal variances assumed	6.156	.017	3.912	46	.000	.10129	.02589	.04917	.15340
	Equal variances not assumed			4.098	45.808	.000	.10129	.02472	.05152	.15105
GPH 2017 P1	Equal variances assumed	2.003	.164	3.151	44	.003	.09754	.03096	.03515	.15993
	Equal variances not assumed			3.427	43.083	.001	.09754	.02846	.04015	.15494
GPH 2017 P2	Equal variances assumed	6.272	.016	2.578	45	.013	.09945	.03858	.02175	.17716
	Equal variances not assumed			2.914	41.340	.006	.09945	.03413	.03054	.16837